Research Square

Preprints are preliminary reports that have not undergone peer review.
They should not be considered conclusive, used to inform clinical practice,
or referenced by the media as validated information.

HDAC1 K438 Lactylation is Associated with NF-κB-related Microglial Inflammatory Activation in Alzheimer's Disease

Xuechao Fei
Chinese Academy of Medical Sciences & Peking Union Medical College
Xue Wang
Chinese Academy of Medical Sciences & Peking Union Medical College
Jiayi Zhang
Academy of Military Medical Sciences
Fan Liu
Chinese Academy of Medical Sciences & Peking Union Medical College
Lingling Zhu
Academy of Military Medical Sciences
Chao Ma
machao@ibms.cams.cn

Chinese Academy of Medical Sciences & Peking Union Medical College

Research Article

Keywords: Alzheimer's disease, Lactylation, Microglia, HDAC1, Neuroinflammation

Posted Date: November 9th, 2026

DOI: https://doi.org/10.21203/rs.3.rs-11455705/v1

License: This work is licensed under a Creative Commons Attribution 4.0 International License.
Read Full License

Additional Declarations: No competing interests reported.

Abstract

Alzheimer's disease (AD) is characterized by persistent microglial activation, yet how metabolic stress contributes to inflammatory reprogramming remains unclear. This study investigated the role of histone deacetylase 1 (HDAC1) lactylation in microglial inflammation. HDAC1 and global protein lactylation were examined in human AD prefrontal cortex and 5×FAD mice, alongside human single-nucleus and spatial transcriptomic analyses. Proteomic and lactylomic profiling of BV2 microglia exposed to hypoxia and lipopolysaccharide (LPS-Hy) was used to characterize inflammatory reprogramming and identify candidate HDAC1 lactylation sites, followed by molecular docking and mutagenesis. HDAC1 lactylation and global protein lactylation signals were elevated in IBA1-positive microglia in human AD tissue and 5×FAD mice and associated with activation markers. Transcriptomic analyses revealed no corresponding increase in HDAC1 mRNA in AD microglia, implicating post-translational modification in HDAC1-associated inflammatory regulation. Lactylomic profiling identified K438 as a major HDAC1 lactylation site, while molecular docking suggested structural compatibility between lactate and the HDAC1 catalytic pocket. Wild-type HDAC1 enhanced LPS-Hy-induced *Il1b* and *Nos2* expression, whereas the K438R mutant abolished detectable HDAC1 lactylation and lost this enhancing effect, accompanied by altered total p65 abundance. Cross-dataset integration identified a conserved immune–metabolic microglial module across human AD, Aβ-positive microglia, and LPS-Hy-treated BV2 cells, with HDAC1 as a highly connected network hub. Together, these findings support a role for HDAC1 K438 lactylation in regulating microglial inflammatory responses under metabolic and inflammatory stress, highlighting a potential non-histone post-translational mechanism linking cellular stress to immune-metabolic reprogramming and a candidate target for further investigation in AD.

Introduction

Alzheimer's disease (AD) involves progressive disruption of neuronal homeostasis accompanied by persistent alterations in immune responses within the central nervous system [1]. Among brain-resident immune cells, microglia undergo substantial functional transitions during AD progression and contribute to chronic inflammatory responses, impaired tissue homeostasis, and neuronal dysfunction [1, 2]. Importantly, these pathological states are not merely reactive to ongoing amyloid pathology; rather, their maintenance implies cell-intrinsic regulatory mechanisms that lock microglia into sustained activation [1, 3]. Recent single-cell and metabolic profiling have revealed that AD-associated microglia exhibit coordinated transcriptional and metabolic remodeling, with lactate-related pathways emerging as core components of this dysfunctional program [4, 5]. Lactate, however, is not merely a glycolytic byproduct; in the AD microenvironment, it acts as a signaling metabolite capable of modulating inflammatory responses. The transduction step remains poorly defined: how a fluctuating metabolic cue is converted into a durable molecular program that sustains microglial inflammation.

Experimental AD models and human brain analyses have consistently shown that disease-associated microglia do not mount a transient inflammatory burst but instead undergo coordinated reprogramming of inflammatory, phagocytic, and metabolic programs, with altered expression of inflammatory

mediators, phagocytic regulators, and lysosomal genes reflecting adaptive responses to amyloid pathology and neuronal injury [6, 7]. This reprogramming includes enhanced glycolytic activity, increased lactate production, and dysregulated energy utilization, suggesting that metabolic adaptation is integral to the microglial disease state rather than a secondary effect of inflammation [4, 5]. Beyond amyloid-driven activation, the AD microenvironment imposes additional metabolic stress, impaired energy homeostasis, mitochondrial dysfunction, and hypoxic insults linked to vascular abnormalities, each of which can shape microglial functional outcomes [8–14]. Lactate, a key end-product of this glycolytic shift, has received particular attention: it acts not only as a metabolic fuel but also as a signaling molecule that modulates inflammatory responses [15, 12]. More recently, histone lactylation has been identified as a mechanism linking lactate accumulation to transcriptional reprogramming in AD microglia, with H4K12 lactylation driving a glycolysis-dependent positive feedback loop that sustains pro-inflammatory gene expression [16]. This histone-based model, however, operates at the chromatin level and cannot readily explain how lactate signals directly and rapidly engage cytoplasmic signaling cascades such as NF-κB. Although initially characterized as a histone mark, lactylation has been found to occur on non-histone proteins involved in transcriptional regulation and intracellular signaling [17–22]. This gap points to a specific unresolved issue: whether non-histone regulatory proteins undergo functionally relevant lactylation in AD microglia, and if so, whether this modification provides a direct route from metabolic stress to inflammatory activation.

Among the potential non-histone targets that might fill this transduction gap, histone deacetylase 1 (HDAC1) emerges as a compelling candidate. HDAC1 is a class I deacetylase with established roles in neuroinflammation: it modulates NF-κB signaling through direct deacetylation of the p65 subunit at Lys310, a modification that controls p65 nuclear translocation and transcriptional activity [23, 24]. Beyond this canonical deacetylase function, HDAC1 also possesses lysine delactylase activity, placing it at the intersection of acetylation and lactylation regulatory networks [25]. In AD, however, the relationship between HDAC1 and disease pathology is not straightforward. Postmortem studies have reported that HDAC1 protein levels decrease in end-stage AD frontal cortex yet increase in mild cognitive impairment, suggesting stage-dependent fluctuations rather than a monotonic decline [26, 27]. In vivo PET imaging further revealed reduced class I HDAC availability in AD patients, correlating inversely with amyloid β (Aβ) and tau burden [28]. Critically, single-nucleus and spatial transcriptomic analyses consistently show that HDAC1 mRNA remains unchanged in AD microglia across cortical regions, indicating that HDAC1 dysregulation in this cell type is unlikely to be driven by transcriptional control. This transcriptional stability, juxtaposed with stage-dependent protein changes, points to post-translational modification as a plausible regulatory layer. Our prior lactylome profiling in BV2 microglia identified HDAC1 as a lactylated component of the nucleosome remodeling and deacetylase (NuRD) complex, but the responsible residue and its functional consequences for inflammatory signaling remained undefined [13]. Given that HDAC1 can be lactylated at specific lysines in other cellular contexts, a modification that alters its epigenetic regulatory activity [29], we therefore investigated whether HDAC1 undergoes disease-associated lactylation in AD microglia and whether this modification directly couples metabolic stress to NF-κB-dependent inflammation.

In the present study, we tested the hypothesis that HDAC1 lactylation at a specific lysine residue couples metabolic stress to NF-κB-dependent microglial inflammation in AD. To address this question, we integrated human AD transcriptomic datasets, 5×FAD mouse models, hypoxic-inflammatory microglial activation paradigms, and quantitative lactylome profiling. Guided by our prior observation that HDAC1 is lactylated within the NuRD complex, we performed site-directed mutagenesis to interrogate the functional contribution of individual lactylation sites to inflammatory signaling. We predicted that mutation of the principal lactylation-responsive residue would abrogate HDAC1-dependent enhancement of inflammatory gene expression and disrupt the HDAC1-p65 regulatory axis. This work identifies HDAC1 K438 lactylation as a metabolically responsive post-translational modification that sustains pro-inflammatory microglial states in AD, and positions this modification as a potential node for therapeutic intervention in neuroinflammation.

METHODS

Participants

Postmortem frozen frontal cortex tissues from AD patients and age-matched controls were obtained from the National Human Brain Bank for Development and Function, Institute of Basic Medical Sciences, Chinese Academy of Medical Sciences (CAMS), which provided demographic, cognitive, and neuropathological data for all cases. The study was approved by the Institutional Review Board of the Institute of Basic Medical Sciences, Chinese Academy of Medical Sciences (Approval No. 009-2014 and 2022125), and written informed consent was obtained from all donors or their next of kin. Donors were included if aged ≥ 50 years with complete clinical and neuropathological information and a postmortem interval ≤ 24 h. Exclusion criteria comprised coexisting neurodegenerative diseases, acute cerebrovascular death, CNS tumors or infections, severe trauma, marked autolysis or tissue artifacts, severe small vessel disease or non-AD tauopathies as dominant pathology, and missing key clinical or neuropathological data. Across three experimental batches, 54 control samples and 75 AD samples were included. Subsets were used for lactate/LDH activity assays (34 control and 61 AD samples), cytokine quantification (10 control and 9 AD samples), and immunoblotting/immunoprecipitation (Supplementary Table 1).

Biochemical measurements of lactate levels and lactate dehydrogenase activity

Frozen brain tissues were homogenized in cold lysis buffer and centrifuged at 12,000 × g for 30 min at 4°C; supernatants were collected for biochemical assays. Lactate concentration was measured by endpoint colorimetry (Beyotime S0208S; A = 450 nm), and LDH activity was determined with a commercial kit (Beyotime P0393S; A = 450 nm). All measurements were normalized to total protein concentration, quantified by bicinchoninic acid assay (Solarbio PC0020; A = 562 nm).

Neuropathological scoring and statistical correlation analysis

Neuropathological severity was assessed using the ABC scoring system (Braak stage and Thal phase) according to published criteria [30]. Spearman correlation analysis was applied to lactate levels, LDH activity, and neuropathological indices.

Enzyme-linked immunosorbent assay

Inflammatory cytokines in human brain homogenates were quantified by ELISA (R&D Systems) using the following kits: CCL4 (DMB00), CCL5 (DY278), CXCL9 (DCX900), IL-1β (DY201), IL-6 (D6050B), TNF-α (DTA00D), and IL-10 (D1000B). Optical density was measured on a microplate reader, and cytokine concentrations were derived from standard curves.

Western blot and immunoprecipitation

Western blot and immunoprecipitation
Protein samples were separated by SDS-PAGE and transferred to PVDF membranes. Membranes were blocked and incubated with primary antibodies against IL-1β (Proteintech, 16806-1-AP), NF-κB p65 (Proteintech, 80979-1-RR), phospho-p65 Ser536 (Proteintech, 80379-2-RR), HIF-1α (Proteintech, 20960-1-AP), β-actin (Proteintech, 66009-1-Ig), Flag (Proteintech, 66008-4-Ig), HDAC1 (Proteintech, 10197-1-AP), and pan-lactyl-lysine (PTM Biolabs, PTM-1401RM), followed by HRP-conjugated secondary antibodies (Abbkine, A25022 and A25012). Signals were visualized by enhanced chemiluminescence. For immunoprecipitation, brain lysates were incubated with anti-Flag or anti-HDAC1 antibodies overnight at 4℃, then with protein A/G agarose beads (Beyotime, P2179M). Immunoprecipitated proteins were eluted and analyzed by immunoblotting with the indicated antibodies.

Immunofluorescence staining and image analysis

Nine-month-old 5×FAD mice and age-matched C57BL/6J controls were obtained from SPF (Beijing) Biotechnology. Animals were housed under specific pathogen-free conditions (12 h light/dark cycle, 26 ℃) with free access to food and water. For tissue collection, mice were deeply anesthetized and perfused transcardially with ice-cold saline followed by 4% paraformaldehyde; brains were post-fixed, paraffin-embedded, and sectioned. Sections were stained with antibodies against HDAC1 (1:100), pan-Kla (1:50), and IBA1 (1:200) using a triple immunofluorescence kit (ImmunoWay Biotechnology). Images were acquired on an Olympus FV1000MPE confocal microscope, and fluorescence intensity and colocalization were quantified with FIJI software. All animal procedures were approved by the Animal Care and Use Committee of the Institute of Basic Medical Sciences, Chinese Academy of Medical Sciences & School of Basic Medicine, Peking Union Medical College (Approval No. ACUC-XMSB-2026-063).

BV2 microglial cell culture and treatments

BV2 microglial cells were obtained from the National Biomedical Cell-Line Resource and maintained in DMEM/F12 (Gibco, 12634010) supplemented with 10% fetal bovine serum (Gibco, A5669201) at 37°C in 5% CO_2. Cells were transfected with HDAC1 wild-type, mutant constructs, or siRNAs (Youbio) using Lipofectamine 3000 (Thermo Fisher Scientific, L3000001).

For hypoxic inflammatory stimulation, cells were exposed to 1% O_2 (Baker Ruskinn Invivo$_2$ system) in the presence of LPS (100 ng/mL; Sigma-Aldrich, L2630) for 24 h (LPS-Hy model)[13]. For real-time impedance monitoring, cells were seeded at 5×10^3 cells/mL or 1×10^4 cells/mL and continuously tracked on the xCELLigence RTCA system. For migration and morphological assays, the initial seeding density was standardized at 1×10^4 cells/mL, and all assessments were performed at 24 h post-stimulation, corresponding to the log-phase growth plateau identified by RTCA. Wound closure and process outgrowth were quantified with FIJI software.

RNA extraction and RT-qPCR

Total RNA from BV2 cells was extracted with TransZol reagent (TransGen Biotech, ET111-01-V2). RNA was reverse-transcribed using a cDNA synthesis kit (Vazyme, R323-01), and qPCR was run with SYBR Green master mix (Vazyme, Q321-02) on a Bio-Rad CFX96 system under the following conditions: 95°C for 3 min; 39 cycles of 95°C for 10 s and 65°C for 33 s; 65°C for 5 s; and 95°C for melt-curve analysis. Primer sequences are provided in Supplementary Table 2. Relative gene expression was calculated by the $2^{-}\Delta\Delta$Ct method.

Molecular docking of L-lactate into the HDAC1 catalytic pocket

The predicted three-dimensional structure of human HDAC1 (UniProt Q13547; AlphaFold AFQ13547-F1-mold.pdb) was retrieved from the AlphaFold Protein Structure Database. L-lactate was docked into the HDAC1 catalytic domain using AlphaFold3, Boltz-2, and Protenix-v2 platforms. Predicted binding poses were compared with the acetate-bound conformation in the experimental HDAC1 structure (PDB: 4BKX).

Public dataset acquisition and preprocessing

Single-nucleus RNA-seq (snRNA-seq) datasets were retrieved from GEO (GSE146639) and from a published early-AD cortical cohort [31]. We also integrated proteomic and lactylation datasets from our previous neuroinflammation study for multi-omics comparison. For microglial nuclei, raw counts were normalized using SCTransform, and batch effects across sequencing runs were corrected with Harmony. Differential expression was called by MAST, applying a false-discovery rate (FDR) < 0.05 and $\log_2$ fold-change > 0.25. For pathway-level interrogation, we queried gene ontology (GO) and kyoto

encyclopedia of genes and genomes (KEGG) annotations for functional enrichment and performed gene set enrichment analysis (GSEA) using the fgsea package with an FDR threshold of 0.1. Routine enrichment analyses were run on the Sangerbox platform (http://www.sangerbox.com/tool) [32]; visualizations were generated with ggplot2 (v3.5.0). Protein-protein interaction networks were built with STRING (v12.0, confidence score ≥ 0.4) and laid out in Cytoscape 3.10.3 using the force-directed layout. Transcription factor-target regulatory networks were inferred from the TRRUST database to map upstream regulators of differentially lactylated proteins. For multiple hypothesis testing, we applied the Benjamini-Hochberg procedure globally. All bioinformatic analyses are detailed in the figure legends and supplementary methods.

Statistical analysis

Statistical analyses were performed using GraphPad Prism 8.0, SPSS 20.0 and R 4.4.2. Data are presented as mean ± SD. Two-group comparisons were performed using an unpaired Student's *t*-test or Mann-Whitney *U* test, as appropriate. Multiple-group comparisons were performed using one-way ANOVA with post hoc tests. Correlations were assessed using Spearman's rank correlation test. Because age differed between the AD and control groups, ANCOVA was used to assess group differences in brain lactate levels and LDH activity after adjustment for age. Log10-transformed values were used as the dependent variables, with group as a fixed factor and age as a covariate. Group-by-age interactions were first tested to assess differences in regression slopes between groups. When the interaction was not significant, the model was refitted without the interaction term to estimate age-adjusted group differences. A two-tailed p value < 0.05 was considered statistically significant.

RESULTS

HDAC1 K438 Lactylation Regulates NF-κB-associated Microglial Inflammation under Metabolic Stress in Alzheimer's Disease

Postmortem prefrontal cortex tissues from patients with AD and controls were analyzed using biochemical assays (Fig. 1A). Across the full cohort of 95 individuals, Spearman's rank correlation analysis revealed a weak positive correlation between age and brain lactate levels (r = 0.276, p = 0.007, Fig. 1B). Lactate levels were higher in AD tissues than in controls in the unadjusted group comparison (Fig. 1C). Given the age difference between the two groups, we performed an ANCOVA to assess the group difference after age adjustment. The group-by-age interaction was not significant (p = 0.209), providing no evidence of a significant difference in the age-lactate regression slopes between groups. After adjustment for age, the difference in log10-transformed lactate levels was no longer statistically significant (p = 0.953, Fig. 1D). These findings suggest that the higher lactate levels observed in AD tissues may be substantially influenced by the age difference between groups, with no statistically significant group difference remaining after age adjustment. Lactate dehydrogenase (LDH) activity showed a decreasing trend in AD tissues compared with controls (Fig. 1E). However, after adjustment

for age, the difference in log10-transformed LDH activity between groups was not statistically significant (p = 0.951, Fig. 1F). ELISA analysis revealed significantly elevated levels of CCL4, CXCL9, IL-1β, IL-6, TNF-α, and IL-10 in AD tissues, while CCL5 remained unchanged (Fig. 1G). Immunoblot analysis further showed significant increases in IL-1β, total p65, and phospho-NF-κB p65 (Ser536) protein levels in AD samples. In contrast, HIF-1α levels and the phospho-p65/total p65 ratio did not differ significantly between groups (Fig. 1H). These findings support an inflammatory state in the AD prefrontal cortex, accompanied by changes in NF-κB pathway-associated protein levels. HIF-1α showed a trend toward increase but did not reach statistical significance in bulk AD cortical tissue (Fig. 1H), arguing against global HIF-1α accumulation in end-stage AD cortex. This does not exclude localized, transient, or microglia-specific HIF-1α stabilization, which bulk postmortem tissue may not resolve. We next examined global protein lactylation and HDAC1-associated lactylation. Immunoblot analysis revealed significantly elevated global protein lactylation (pan-Kla) in AD brains (Fig. 1I). Immunofluorescence staining further showed enrichment of pan-Kla signals in HDAC1-positive $IBA1^+$ microglia in AD cortex (Fig. 1J). Consistently, immunoprecipitation of HDAC1 from brain lysates revealed increased HDAC1-associated lactylation in AD samples compared with controls (Fig. 1K). Collectively, these findings associate increased HDAC1 lactylation with inflammatory changes in the AD brain, although the higher bulk tissue lactate levels observed in the unadjusted comparison did not remain significantly different after adjustment for age.

(A) Postmortem prefrontal cortex tissues from control and AD subjects were homogenized and centrifuged; supernatants were collected for lactate concentration and LDH activity measurements. **(B)** Correlation between prefrontal cortex lactate levels and age across the entire cohort. **(C)** Comparison of prefrontal cortex lactate levels between control and AD donors. **(D)** Age-adjusted comparison of lactate levels between control and AD donors using ANCOVA. Data points represent estimated marginal means (EMMs), and error bars indicate 95% confidence intervals (CIs). **(E)** Comparison of LDH activity between control and AD donors. **(F)** Age-adjusted comparison of LDH activity between control and AD donors using ANCOVA. Data points represent EMMs, and error bars indicate 95% CIs. **(G)** Quantification of inflammatory cytokines and chemokines (CCL4, CXCL9, IL-1β, IL-6, TNF-α, and IL-10) in prefrontal cortex homogenates from control and AD donors. **(H)** Representative immunoblots and densitometric analyses of HIF-1α, IL-1β, phospho-NF-κB p65 (Ser536), and total p65 in control and AD prefrontal cortex. **(I)** Representative immunoblot and quantification of global protein lactylation (pan-Kla). **(J)** Representative immunofluorescence staining of IBA1 (red), HDAC1 (yellow), pan-Kla (green), and DAPI (blue) in control and AD prefrontal cortex; right panels display fluorescence intensity profiles along the indicated lines. **(K)** Immunoprecipitation of HDAC1 from prefrontal cortex lysates, followed by immunoblotting with anti-Kla antibody and densitometric quantification. Data are presented as mean ± SD, except for age-adjusted EMMs, which are shown with 95% CIs. *p < 0.05, **p < 0.01, ***p < 0.001; ns, not significant.

AD-associated microglia exhibit a conserved immune-metabolic transcriptional program across cortical regions

We integrated two independent single-cell RNA-seq datasets derived from distinct cortical areas, frontal cortex microglia [31] and microglia from superior parietal and superior frontal regions [33], to identify conserved disease-associated transcriptional features that persist across anatomical locations. In the frontal cortex dataset, KEGG analysis highlighted prominent enrichment of canonical inflammatory pathways, HIF-1 signaling, NF-κB signaling, TNF signaling, and MAPK signaling, together with innate immune activation modules such as Toll-like receptor and NOD-like receptor signaling (Fig. 2A). GO enrichment analyses further revealed a coordinated shift in molecular functions related to cytokine receptor activity, NF-κB-associated transcriptional regulation, and redox-sensitive enzyme activity, accompanied by biological processes reflecting sustained immune activation and cellular responses to hypoxic stress (Fig. 2B). This pattern of transcriptional reprogramming was independently replicated in the second cortical dataset, where similar enrichment of Toll-like receptor signaling, cytokine-cytokine receptor interaction, and JAK-STAT signaling was observed (Fig. 2D-E). Differential expression analysis across both datasets revealed broad reconfiguration of microglial gene programs in AD (Fig. 2C). Rather than isolated gene changes, the overall expression landscape reflected a polarized state with coordinated activation and repression of functional modules. Critically, HDAC1 expression remained unchanged at the transcriptional level across all conditions. This transcriptional stability was confirmed by spatial transcriptomic analysis of the human hippocampal AD dataset, which showed no significant alteration of HDAC1 expression in hippocampal microglia (Fig. S1) [10]. Thus, while AD-associated microglia exhibit a conserved and robust inflammatory-hypoxic transcriptional state, HDAC1 dysregulation in this cell type is not driven by changes in transcript abundance. These observations point instead to post-translational regulation of HDAC1 as the relevant functional layer.

HDAC1 lactylation is increased in activated microglia and associates with inflammatory programs in AD mice

Immunofluorescence staining of cortical sections from 5×FAD mice revealed increased IBA1$^+$-pan-Kla$^+$ microglia compared with wild-type controls. Within IBA1$^+$ cells, HDAC1 immunoreactivity was elevated and showed enhanced co-localization with pan-Kla signals (Fig. 3A). Quantitative fluorescence intensity analysis confirmed increased spatial overlap between HDAC1 and pan-Kla in 5×FAD cortex, indicating elevated HDAC1 lactylation under AD conditions. This observation was consistent in hippocampal CA1 sections from independent experimental batches (Fig. S2), supporting the robustness of the finding across brain regions. Consistent with the transcriptional state identified in AD-associated microglia (Fig. 2), GO and KEGG enrichment analyses of upregulated microglial genes in 5×FAD mice revealed coordinated activation of inflammatory, immune, and stress-response programs (Fig. 3B). Biological process terms were dominated by positive regulation of inflammatory response, leukocyte chemotaxis, and neuroinflammatory processes; molecular function terms highlighted cytokine and chemokine receptor binding, NF-κB-associated functions, and oxidoreductase activity; and cellular component enrichment pointed to lysosomal, phagocytic, and mitochondrial compartments. KEGG analysis further confirmed enrichment of Toll-like receptor, NF-κB, MAPK, JAK-STAT, TNF, and HIF-1 signaling pathways.

Together, these data confirm that 5×FAD microglia undergo a conserved inflammatory-hypoxic activation program that mirrors the transcriptional state observed in human AD microglia.

Hypoxic inflammatory stimulation induces AD-like microglial proteomic reprogramming

We exposed BV2 microglia to 1% O_2 combined with LPS (LPS-Hy) to model combined inflammatory and hypoxic/metabolic stress that microglia may encounter in the AD microenvironment. Real-time cell impedance analysis (RTCA) revealed a dynamic increase in cell index following LPS-Hy stimulation, with a peak at approximately 17 h post-seeding and a gradual decline thereafter (Fig. 4A). Based on these kinetics, all morphological and migration assessments were performed at 24 h post-intervention. Under LPS-Hy, BV2 microglia showed significantly accelerated wound closure compared with control conditions, consistent with enhanced migratory capacity (Fig. 4B), and morphological analyses revealed pronounced process outgrowth and elongation, indicating microglial activation (Fig. 4C).

Proteomic profiling revealed extensive remodeling of the microglial proteome under LPS-Hy stimulation. Upregulated proteins were predominantly associated with inflammatory and innate immune activation programs, including COX-2, Cd14, Irg1, and ADAP, reflecting enhanced prostaglandin metabolism, pattern recognition receptor signaling, and cytoskeleton-associated immune activation. In parallel, proteins involved in DNA replication and canonical cell-cycle regulation-Ki-67, Np95, Brip1, and related chromatin maintenance factors-were downregulated, suggesting a reprogramming away from proliferative cell-cycle machinery toward an activated immune effector state (Fig. 4D). Gene set enrichment analysis (GSEA) further confirmed activation of immune and stress-response pathways, including Toll-like receptor signaling, leukocyte transendothelial migration, NOD-like receptor signaling, VEGF signaling, and insulin-related metabolic pathways (Fig. 4E). Functional enrichment of upregulated proteins highlighted biological processes related to phagocytosis, response to external stimuli, and regulation of innate immune activation, together with molecular functions such as cytokine binding, ubiquitin-like protein binding, and receptor-mediated signaling (Fig. 4F-G). KEGG analysis pointed to enrichment of MAPK signaling, Fc gamma R-mediated phagocytosis, endocytosis, and ubiquitin-mediated proteolysis (Fig. 4G). Conversely, downregulated proteins were enriched in pathways associated with cell cycle regulation, DNA replication, mismatch repair, and nucleotide metabolism, with KEGG analysis highlighting cell cycle control, p53 signaling, and DNA repair programs (Fig. 4H-I). PPI and transcription factor prediction analyses identified interconnected networks among these differentially expressed proteins, linking upregulated proteins to inflammatory- and hypoxia-associated transcriptional programs (RELA, NFKB1, HIF1A, STAT3) and downregulated proteins to cell-cycle-related regulatory networks (Fig. S3A-B). Within this framework, HDAC1 emerged as a candidate transcription factor in the upregulated regulatory network, consistent with its reported roles in epigenetic and inflammatory regulation. Collectively, these analyses suggest that hypoxic-inflammatory stimulation induces coordinated proteomic reorganization accompanied by transcriptional regulatory rewiring, in which HDAC1 may function as a context-dependent epigenetic modulator.

Lactylome profiling identifies HDAC1 K438 as a candidate regulatory lactylation site in microglial reprogramming

We next turned to lactylome profiling of BV2 microglia following LPS-Hy stimulation to identify lactylation-dependent regulatory remodeling. Global pathway analysis of lactylated proteins revealed significant enrichment in processes related to ribosome biogenesis, protein translation, and cytoskeletal organization, together with alterations in tight junction-associated pathways, whereas signaling pathways such as Wnt and Notch were comparatively reduced (Fig. 5A-E). Functional enrichment analysis of significantly upregulated lactylated proteins further demonstrated strong association with chromatin organization, transcriptional regulation, histone modification complexes, RNA binding, and chromatin-associated regulatory functions across GO biological process, molecular function, and cellular component categories (Fig. 5F-H). Pathway association analysis linked upregulated lactylated proteins to major inflammatory and stress-response signaling cascades, including NF-κB, HIF-1, MAPK, VEGF, Toll-like receptor, TNF, and JAK-STAT pathways (Fig. 5I). While these broad enrichments confirmed that lactylation broadly engages inflammatory and stress-response programs in activated microglia, they did not identify which specific lactylated proteins might serve as functional regulatory nodes. We therefore examined lactylation events on individual proteins, focusing on HDAC1 based on its established roles in epigenetic and inflammatory regulation. Site-specific lactylome profiling identified multiple significantly altered lactylation sites on HDAC1 following LPS-Hy stimulation. Among the detected lysine residues (K412, K432, K438, K444, and K473) K438 exhibited the strongest lactylation response (Fig. 5J-K). Structural mapping placed K438 within a conserved regulatory region enriched for post-translational modification hotspots, suggesting potential functional relevance in modulating HDAC1 activity during inflammatory stress (Fig. 5L). These data point to K438 as the principal lactylation site on HDAC1 in this setting and set the stage for functional interrogation of this modification.

To further examine whether HDAC1 possesses a structural basis for interacting with lactate, we performed molecular docking of L-lactate into the HDAC1 catalytic pocket. Three independent prediction platforms (AlphaFold3, Boltz-2, and Protenix-v2) converged on a consistent lactate binding pose within the conserved catalytic pocket, with the ligand carboxyl group coordinating the catalytic Zn^{2+} ion. The predicted lactate poses from all three models overlapped with each other and with the acetate product position in the experimental HDAC1 structure (4BKX) (Fig. S4). This convergence across independent models supports a structural compatibility between lactate and the HDAC1 active site.

HDAC1 K438 lactylation regulates NF-κB-mediated inflammatory activation in microglia

To test whether K438 is functionally relevant for HDAC1-mediated inflammatory regulation, we first knocked down endogenous HDAC1 in BV2 microglia under LPS-Hy conditions (Fig. S5A-B). HDAC1 depletion produced a bifurcated transcriptional response: *Il1b*, *Il6* and *Nos2* (also known as *Nos2*) mRNA rose sharply, whereas *Ccl4* and *Ccl5* mRNA dropped; *Tnf* mRNA was unaffected (Fig. 6A). This pattern

implies that endogenous HDAC1 exerts gene-specific, rather than global, suppression of inflammatory programs. Wild type HDAC1 (wt-HDAC1) overexpression recapitulated the pro-inflammatory effect on *Il1b* and *Nos2*. Critically, the K438R mutant ablated this induction, *Il1b* and *Nos2s* mRNA fell back to near-vector-control levels, while *Tnf*, *Ccl4*, and *Ccl5* mRNA rebounded significantly above wild type-overexpressing cells (Fig. 6B). Thus, K438 is dispensable for basal HDAC1 expression but obligatory for its enhancing effect on a specific NF-κB-related transcriptional cluster (*Il1b/ Nos2* mRNA), and its mutation paradoxically relieves repression on chemokine genes.

At the signaling level, wt-HDAC1 overexpression did not alter total p65 abundance, whereas K438R increased total p65 protein without affecting phospho-p65 occupancy (Fig. 6C). This unexpected observation suggests that the K438R mutation may affect p65 stability rather than its phosphorylation state. Immunoprecipitation of Flag-tagged HDAC1 confirmed that LPS-Hy-induced lactylation was robust on wild type but nearly undetectable on K438R (Fig. 6D), formally linking the K438 residue to the bulk of HDAC1-associated lactylation in this setting. Together, these data demonstrate that K438 is required for HDAC1's enhancing effect on *Il1b* and *Nos2* mRNA expression and that its loss does not simply eliminate HDAC1 activity but may reroute it toward alternative transcriptional outputs.

Conserved microglial module with HDAC1-linked regulation in AD and inflammatory stress

We therefore integrated three complementary datasets, single-cell RNA-seq from AD-associated microglia (AD-MG) [33] and Aβ-positive microglia ($Aβ^+$-MG) [31], together with proteomic profiling of BV2 microglia exposed to LPS-Hy, to identify cross-species molecular programs shared across human AD and experimental inflammatory stress. Cross-modal integration revealed eight robustly conserved factors across species: ATP1B3, ATP6V1E1, CD9, GPNMB, LGALS3, PFKP, STAT1, and 14-3-3 epsilon (Fig. 7A). This minimal core module was consistently observed across human disease states and experimental conditions, suggesting a fundamental microglial adaptation program. These core genes exhibited coordinated regulation across transcriptomic and proteomic layers (Fig. 7B). To examine whether HDAC1 participates in the conserved module's interaction network, we performed a STRING-based PPI expansion using the eight core genes as seeds to retrieve experimentally supported interactors. Within this extended network, cytoHubba topological ranking identified STAT1, EGFR, and ANXA5 as top core factors, depicted as green nodes (Fig. 7C). Notably, without any prior weighting, HDAC1 naturally arose as a highly connected hub, bridging metabolic and inflammatory signaling components. Edge thickness and color in the network reflect experimentally determined interaction confidence, providing a stringent measure of physical connectivity (Fig. 7C). This emergent connectivity places HDAC1 within a cross-species conserved microglial adaptation network rather than an isolated axis, consistent with its functional role in inflammatory reprogramming demonstrated earlier. Together, these data identify a cross-species conserved microglial core module that links inflammatory activation and metabolic adaptation across human AD pathology and experimental inflammatory stress, and position HDAC1 as a context-integrated regulatory component within this network.

DISCUSSION

Our data support a model in which HDAC1 K438 lactylation, characterized in LPS-Hy microglia, may contribute to NF-κB-associated inflammatory activation in AD, while human AD tissue shows elevated HDAC1-associated lactylation. This finding addresses a specific mechanistic gap identified in our introduction: lactate as the transduction step by which a fluctuating metabolic cue is converted into a durable pro-inflammatory program. Prior work established that histone H4K12 lactylation drives glycolytic gene expression in AD microglia, but that mechanism operates at the chromatin level and cannot readily explain how metabolic signals directly engage cytoplasmic inflammatory cascades. In LPS-Hy BV2 microglia, K438 was the principal HDAC1 lactylation site and was required for HDAC1-enhanced *Il1b* and *Nos2* expression, accompanied by altered p65 abundance. Human AD tissue showed increased HDAC1-associated lactylation without a corresponding increase in HDAC1 mRNA. This mechanism is conceptually distinct from histone-based lactylation: rather than reprogramming the metabolic transcriptome, HDAC1 K438 lactylation directly tunes the activity of an inflammatory signaling node, providing a rapid and metabolically responsive route from lactate accumulation to sustained microglial activation.

HDAC1 expression levels in the frontal cortex are decreased in advanced AD, but increased in mild cognitive impairment [26, 27]. The stage-dependent fluctuations, together with PET evidence showing reduced class I HDAC availability that correlates inversely with Aβ and tau burden [28], suggest that HDAC1 dysregulation follows a dynamic trajectory rather than a monotonic loss. This trajectory raises the possibility that HDAC1 may exert opposing effects at different disease stages, consistent with the context-dependent functions of class I HDACs in microglia [40]. Adding to this complexity, transcriptomic network analyses have positioned HDAC1 as a hub gene in AD-associated co-expression modules [41–44]. These observations share a common limitation: they focus on HDAC1 abundance or net availability, neither of which captures the functional state of the enzyme. In this study, HDAC1 mRNA remained unchanged in AD microglia, whereas HDAC1-associated lactylation was elevated in AD cortical tissue; in LPS-Hy-stimulated BV2 microglia, K438 was the principal lactylation-responsive site on HDAC1. Together, these findings dissociate HDAC1 dysregulation from transcriptional control and instead link it to metabolism-dependent post-translational modification.

Our finding that HDAC1 K438 lactylation modulates NF-κB-associated inflammatory gene expression and p65 regulation in LPS-Hy microglia adds a new modality to the growing repertoire of functionally relevant lactylation events in AD. Pan and colleagues showed that H4K12 lactylation is elevated in plaque-associated microglia, where it drives a glycolysis/PKM2 positive feedback loop that sustains pro-inflammatory activation [16]. This histone-based mechanism operates at the chromatin level to reprogram metabolic gene expression and may act in parallel with the HDAC1 K438 pathway described here: the former sustains the glycolytic engine, whereas the latter redirects its output toward inflammatory effector genes. Subsequent studies have extended lactylation to non-histone substrates, revealing substrate- and site-specific outcomes: APP K612 lactylation promotes amyloidogenic APP trafficking toward endosomal degradation and reduces Aβ pathology [45], whereas tau K331 and K677

lactylation have been implicated in pathogenic tau accumulation and ferritinophagy-dependent ferroptosis [46, 47]. More recently, HDAC1 K412 lactylation was reported in colorectal cancer cells, where it maintains deacetylase activity and confers resistance to ferroptosis [29]. In contrast, our data identify a distinct lactylation event on the same protein. This event occurs in a different cellular context, namely microglia under AD-relevant inflammatory-metabolic stress. It also has a different functional output. Specifically, it is linked to NF-κB-associated inflammatory activation rather than ferroptosis resistance. Whether this site-specific divergence reflects differential recognition by the lactylation machinery (p300/CBP versus AARS1) or differential responsiveness to distinct metabolic cues remains an open question [17]. Together, these observations position HDAC1 K438 lactylation as a context-specific regulatory node that may link metabolic stress to persistent neuroinflammation, adding to a growing list of non-histone lactylation events with substrate- and site-specific functional consequences in AD pathophysiology.

Our data align with and extend a growing view of HDAC1 as a context-dependent regulator whose functional output is shaped by its post-translational modification status. HDAC1 has been shown to modulate NF-κB signaling through direct deacetylation of p65 at Lys310, reducing its transcriptional output [34], and to regulate CREB1 activity through deacetylation at K292 [43]. In ischemic stroke, HDAC1 deficiency promotes a pro-inflammatory microglial phenotype, whereas pharmacological restoration of HDAC1 activity attenuates NF-κB-driven neuroinflammation [34]. These observations position HDAC1 as an endogenous modulator of inflammatory signaling beyond its canonical chromatin-remodeling function. The contextual nature of HDAC1 function is further illustrated by SUMOylation: PIAS1-mediated SUMOylation of HDAC1 at K444 and K476 converts it from a transcriptional repressor into a neuroprotective molecule that promotes Mcl-1 expression and upregulates the Aβ-degrading enzyme neprilysin [48]. Thus, the same enzyme can exert opposing effects depending on its modification status. Our findings add lactylation to this regulatory repertoire, and specifically identify K438 lactylation as a modification that, in the metabolically stressed AD microenvironment, tilts HDAC1 function toward NF-κB-dependent inflammatory activation. This supports a model in which HDAC1 operates as a platform for integrating multiple PTM inputs-acetylation, SUMOylation, and lactylation-each of which may be engaged by distinct cellular cues to produce context-appropriate functional outcomes.

One aspect of our data warrants closer scrutiny. In BV2 microglia overexpressing the K438R mutant, total p65 protein abundance increased without a corresponding change in p65 phosphorylation (Fig. 6C). This finding was unexpected: if K438 lactylation simply enhanced p65-driven transcription, one would not necessarily predict an increase in p65 protein itself. Several non-mutually exclusive interpretations merit consideration. First, K438R mutation may alter the interaction between HDAC1 and the p65 protein, potentially affecting p65 stability through changes in ubiquitination or proteasomal turnover. Second, the lactylation-deficient mutant may exert a dominant-negative effect on endogenous HDAC1, indirectly perturbing p65 homeostasis. Third, our current data do not distinguish whether K438 lactylation directly modifies the HDAC1-p65 physical interaction or acts indirectly through conformational changes that affect HDAC1's association with other regulatory partners. Resolving these possibilities will require orthogonal approaches, including co-immunoprecipitation under native conditions, ubiquitin profiling,

and structure-function analyses. Regardless of the precise mechanism, the functional consequence is clear: K438 lactylation is required for HDAC1's enhancing effect on *Il1b* and *Nos2* mRNA expression, and its loss does not simply eliminate HDAC1 activity but may reroute it toward alternative outputs.

Despite this functional clarity, several experimental limitations should be acknowledged. They fall into three categories: technical constraints, conceptual boundaries, and priorities for causal testing. The LPS-Hy paradigm was used to impose a defined inflammatory-metabolic challenge for mechanistic dissection of HDAC1 lactylation, rather than to reproduce the full metabolic complexity of human AD. The absence of significant HIF-1α accumulation in bulk AD cortex may reflect the limited sensitivity of postmortem bulk tissue to transient, cell-type-specific, or spatially restricted hypoxic signaling. Our human AD cohort and the 5×FAD/BV2 models cannot fully capture the genetic and metabolic heterogeneity of sporadic AD, particularly the age-related metabolic changes that shape microglial phenotypes in humans. Conceptual boundaries: lactylation operates within a broader network of acyl modifications, and we have not systematically assessed whether additional lactylated regulators cooperate with or compensate for HDAC1 K438 in inflammatory control. The most direct test of causality, microglia-specific knock-in of the K438R mutation in an AD mouse model, remains to be generated. Such a model would formally establish whether ablating this single lactylation site is sufficient to attenuate neuroinflammation and, more importantly, whether it modifies cognitive outcomes. Priorities for future work also include spatially resolved lactylome profiling to examine whether K438 lactylation is enriched in plaque-associated versus plaque-distant microglia, and quantitative PTM crosstalk analysis to determine whether K438 lactylation competes with or facilitates nearby modifications on HDAC1. These experiments are feasible and will be essential to translate our mechanistic findings into a therapeutically tractable framework.

The emerging evidence collectively points to lactylation as both a mechanistic driver and a pharmacologically responsive modification in neuroinflammation. In a BV2 microglial setting comparable to this experimental system, sodium oxamate, as an inhibitor of LDHA, lowered lactate availability, reduced global lactylation, and suppressed proinflammatory activation [49]. These observations support the feasibility of pharmacologically intervening in the lactylation-NF-κB cascade. The observations summarized above integrate these findings into a mechanistic hypothesis with several testable features (Fig. 8). Under hypoxic-inflammatory stress, microglia shift toward glycolytic metabolism, with lactate production increasing substantially [50, 13, 51–53]. Lactate is converted to lactyl-CoA, which serves as the acyl donor for p300/CBP-or AARS1- dependent lactylation [54–56]. Within this framework, HDAC1 undergoes lactylation at K438, and this modification, rather than merely altering HDAC1 abundance or chromatin association, directly modulates the HDAC1-p65 interaction, enhances p65-driven transcriptional activity, and promotes expression of pro-inflammatory mediators [57, 34]. The consequence is a feed-forward loop: K438 lactylation reinforces inflammatory gene expression, which in turn sustains microglial activation in the metabolically stressed AD microenvironment. Unlike histone lactylation, which reprograms the metabolic transcriptome over longer timescales, HDAC1 K438 lactylation provides a post-translational route that can engage inflammatory signaling more rapidly and with site-specific precision. This model positions HDAC1 K438 lactylation as

a molecular interface that translates metabolic alterations into a durable inflammatory program, and identifies this modification as a potential point of intervention for disrupting the metabolic-inflammatory axis in AD.

CONCLUSION

Our data support a model in which HDAC1 K438 lactylation acts as a metabolically responsive post-translational modification that contributes to NF-κB-associated microglial inflammation in AD. This mechanism may link lactate-related metabolic stress, to NF-κB-associated microglial inflammatory activation. In human AD cortex, however, lactate and LDH differences were not significant after age adjustment. Accordingly, this link should be interpreted as a model rather than as an established metabolic alteration in end-stage AD. Nevertheless, these findings extend our understanding of HDAC1 regulation beyond expression-level changes. The finding that site-specific lactylation of a non-histone regulatory protein, rather than chromatin-level histone modification, contributes to this effect identifies a conceptually distinct route from metabolic stress to neuroinflammation. Although direct causal evidence in vivo, particularly from microglia-specific K438R knock-in models, remains to be generated, the multi-layered evidence presented here positions HDAC1 K438 lactylation as a candidate target for neuroinflammatory intervention in AD.

Declarations

Acknowledgements

We thank the National Human Brain Bank for Development and Function, Chinese Academy of Medical Sciences, and Peking Union Medical College forsupplying donors' brain tissues.

Fundings

Supported by grants from: STI2030-Major Project #2021ZD0201100 Task 1 #2021ZD0201101.

CRediT authorship contribution statement

Xuechao Fei: Conceptualization, Investigation, Formal analysis, Writing-original draft, Writing-review & editing. **Xue Wang**: Investigation, Formal analysis. **Jiayi Zhang**: Investigation, Data curation. **Fan Liu**: Investigation. **Lingling Zhu**: Conceptualization, Writing-review & editing. **Chao Ma**: Conceptualization, Writing-review & editing.

Data availability

The data used in this study are sourced exclusively from three previously published articles with the following DOIs: 10.1016/j.cell.2023.08.005, 10.3389/fnmol.2020.00134 (including the GEO dataset GSE146639), and 10.1186/s12964-024-01748-x. No newly generated datasets are associated with this study. All data are available from the corresponding publications and their supplementary materials.

Declaration of interest statement

The authors declare no conflict of interest.

References

1. Miao J, Chen L, Pan X, Li L, Zhao B, Lan J (2023) Microglial Metabolic Reprogramming: Emerging Insights and Therapeutic Strategies in Neurodegenerative Diseases. Cell Mol Neurobiol 43(7):3191–3210. 10.1007/s10571-023-01376-y
2. Kong C, Jia L, Jia J (2022) gamma-mangostin attenuates amyloid-beta42-induced neuroinflammation and oxidative stress in microglia-like BV2 cells via the mitogen-activated protein kinases signaling pathway. Eur J Pharmacol 917:174744. 10.1016/j.ejphar.2022.174744
3. Li L, Gu Y, Luo X, Wang J, Jia Y, Yan T (2026) Chrysin reprograms microglial metabolism and function via targeting SYK to alleviate the symptoms of Alzheimer's disease. J Ethnopharmacol 370:122056. 10.1016/j.jep.2026.122056
4. Ashley CC, Constantino NJ, Pettit-Mee RJ, Snipes JA, Saito K, Irmen RE, Zhang R, Neary EM, Lanning MJ, Karch CM, Johnson LA, Morganti JM, Macauley SL (2026) Lactate metabolism links reactive microglia, amyloid pathology, and Abeta dynamics. J Neuroinflamm 23(1). 10.1186/s12974-026-03825-z
5. Liu H, Yi X, You M, Yang H, Zhang S, Huang S, Xie L (2024) Bulk-RNA and single-nuclei RNA seq analyses reveal the role of lactate metabolism-related genes in Alzheimer's disease. Metab Brain Dis 39(7):1469–1480. 10.1007/s11011-024-01396-7
6. Zhang M, Wang W, Ye Q, Fu Y, Li X, Yang K, Gao F, Zhou A, Wei Y, Tian S, Li S, Wei F, Shi W, Li WD (2024) Histone deacetylase inhibitors VPA and WT161 ameliorate the pathological features and cognitive impairments of the APP/PS1 Alzheimer's disease mouse model by regulating the expression of APP secretases. Alzheimers Res Ther 16(1):15. 10.1186/s13195-024-01384-0
7. Kleandrova VV, Speck-Planche A (2020) PTML Modeling for Alzheimer's Disease: Design and Prediction of Virtual Multi-Target Inhibitors of GSK3B, HDAC1, and HDAC6. Curr Top Med Chem 20(19):1661–1676. 10.2174/1568026620666200607190951
8. Li Q, Peng J, Luo Y, Zhou J, Li T, Cao L, Peng S, Zuo Z, Wang Z (2022) Far infrared light irradiation enhances Aβ clearance via increased exocytotic microglial ATP and ameliorates cognitive deficit in Alzheimer's disease-like mice. J Neuroinflamm 19(1):145. 10.1186/s12974-022-02521-y

9. Wen W, Chen J, Xiang J, Zhang S, Liu J, Wang J, Wang P, Xu S (2025) Facilitating microglial phagocytosis by which Jiawei Xionggui Decoction alleviates cognitive impairment via TREM2-mediated energy metabolic reprogramming. Chin J Nat Med 23(8):909–919. 10.1016/S1875-5364(25)60927-7
10. Wang P, Han L, Wang L, Tao Q, Guo Z, Luo T, He Y, Xu Z, Yu J, Liu Y, Wu Z, Xu B, Jin B, Wei Y, Yang Y, Cheng M, Jiang Y, Tian C, Zheng H, Fan Z, Jiang P, Gao Y, Wu J, Wang S, Sun B, Fang Z, Lei J, Luo B, Wen H, Peng G, Tang Y, Yang T, Chen J, Zhuang Z, Su X, Pan C, Zhu K, Shen Y, Liu S, Bao A, Yao J, Wang J, Xu X, Li XM, Liu L, Duan S, Zhang J (2025) Molecular pathways and diagnosis in spatially resolved Alzheimer's hippocampal atlas. Neuron 113 (13):2123–2140 e2129. 10.1016/j.neuron.2025.03.002
11. Deng J, Li Y, Yin L, Liu S, Li Y, Liao W, Mu L, Luo X, Qin J (2025) Histone lactylation enhances GCLC expression and thus promotes chemoresistance of colorectal cancer stem cells through inhibiting ferroptosis. Cell Death Dis 16(1):193. 10.1038/s41419-025-07498-z
12. Wu Y, Wang X, Zhang W, Fu J, Jiang K, Shen Y, Li C, Gao H (2024) Modulation of choline and lactate metabolism by basic fibroblast growth factor mitigates neuroinflammation in type 2 diabetes: Insights from (1)H-NMR metabolomics analysis. Neuropharmacology 257:110049. 10.1016/j.neuropharm.2024.110049
13. Jiang X, Gao J, Fei X, Geng Y, Yue X, Shi Z, Cheng X, Zhao T, Fan M, Wu H, Zhao M, Zhu L (2024) Global profiling of protein lactylation in microglia in experimental high-altitude cerebral edema. Cell Commun Signal 22(1):374. 10.1186/s12964-024-01748-x
14. Lipari CLR, Patti A, Conti-Nibali S, Messina AA, Magri A, Sortino MA, Merlo S (2025) Hypoxia reverses the early anti-inflammatory microglial response to the beta-amyloid peptide: mitochondrial involvement and beneficial roles of melatonin and naringenin. J Transl Med 23(1):1012. 10.1186/s12967-025-07044-7
15. Ashley CC, Constantino NJ, Pettit-Mee RJ, Snipes JA, Saito K, Irmen RE, Zhang R, Neary EM, Lanning MJ, Karch CM, Johnson LA, Morganti JM, Macauley SL (2026) Lactate metabolism links reactive microglia, amyloid pathology, and Aβ dynamics. J Neuroinflamm 23(1). 10.1186/s12974-026-03825-z
16. Pan RY, He L, Zhang J, Liu X, Liao Y, Gao J, Liao Y, Yan Y, Li Q, Zhou X, Cheng J, Xing Q, Guan F, Zhang J, Sun L, Yuan Z (2022) Positive feedback regulation of microglial glucose metabolism by histone H4 lysine 12 lactylation in Alzheimer's disease. Cell Metabol 34(4):634–648e636. 10.1016/j.cmet.2022.02.013
17. Ju J, Zhang H, Lin M, Yan Z, An L, Cao Z, Geng D, Yue J, Tang Y, Tian L, Chen F, Han Y, Wang W, Zhao S, Jiao S, Zhou Z (2024) The alanyl-tRNA synthetase AARS1 moonlights as a lactyltransferase to promote YAP signaling in gastric cancer. J Clin Invest 134(10). 10.1172/JCI174587
18. Wang X, Fan W, Li N, Ma Y, Yao M, Wang G, He S, Li W, Tan J, Lu Q, Hou S (2023) YY1 lactylation in microglia promotes angiogenesis through transcription activation-mediated upregulation of FGF2. Genome Biol 24(1):87. 10.1186/s13059-023-02931-y

19. Mao Y, Zhang J, Zhou Q, He X, Zheng Z, Wei Y, Zhou K, Lin Y, Yu H, Zhang H, Zhou Y, Lin P, Wu B, Yuan Y, Zhao J, Xu W, Zhao S (2024) Hypoxia induces mitochondrial protein lactylation to limit oxidative phosphorylation. Cell Res 34(1):13–30. 10.1038/s41422-023-00864-6
20. Wang J, Yang P, Yu T, Gao M, Liu D, Zhang J, Lu C, Chen X, Zhang X, Liu Y (2022) Lactylation of PKM2 Suppresses Inflammatory Metabolic Adaptation in Pro-inflammatory Macrophages. Int J Biol Sci 18(16):6210–6225. 10.7150/ijbs.75434
21. Wang L, Li D, Yao F, Feng S, Tong C, Rao R, Zhong M, Wang X, Feng W, Hu Z, Jin B, Wang L, Hu S, Zhou B (2025) Serpina3k lactylation protects from cardiac ischemia reperfusion injury. Nat Commun 16(1):1012. 10.1038/s41467-024-55589-w
22. Chen H, Li Y, Li H, Chen X, Fu H, Mao D, Chen W, Lan L, Wang C, Hu K, Li J, Zhu C, Evans I, Cheung E, Lu D, He Y, Behrens A, Yin D, Zhang C (2024) NBS1 lactylation is required for efficient DNA repair and chemotherapy resistance. Nature 631(8021):663–669. 10.1038/s41586-024-07620-9
23. Peng Y, Xiong RP, Wang B, Chen X, Ning YL, Zhao Y, Yang N, Zhang J, Li CH, Zhou YG, Li P (2025) c-Ski is a novel repressor of NF-κB through interaction with p65 and HDAC1 in U937 cells. Cell Commun Signal 23(1):165. 10.1186/s12964-025-02178-z
24. Peng Y, Liu B, Xu S, Qu R, Zhang R, Wang C, Liu Y, Wei H, Tian Q, Zhang M, Bi H, Yin X, Guo D (2026) miR-223-3p improves macrophage polarization balance and mitochondrial metabolism to ameliorate uveitis by orchestrating P65(Lys310) acetylation through RBPJ/HDAC1 axis. Cell Mol Biol Lett 31(1). 10.1186/s11658-026-00874-3
25. Moreno-Yruela C, Zhang D, Wei W, Bæk M, Liu W, Gao J, Danková D, Nielsen AL, Bolding JE, Yang L, Jameson ST, Wong J, Olsen CA, Zhao Y (2022) Class I histone deacetylases (HDAC1-3) are histone lysine delactylases. Sci Adv 8(3):eabi6696. 10.1126/sciadv.abi6696
26. Schueller E, Paiva I, Blanc F, Wang XL, Cassel JC, Boutillier AL, Bousiges O (2020) Dysregulation of histone acetylation pathways in hippocampus and frontal cortex of Alzheimer's disease patients. Eur Neuropsychopharmacol 33:101–116. 10.1016/j.euroneuro.2020.01.015
27. Mahady L, Nadeem M, Malek-Ahmadi M, Chen K, Perez SE, Mufson EJ (2018) Frontal Cortex Epigenetic Dysregulation During the Progression of Alzheimer's Disease. J Alzheimer's disease: JAD 62(1):115–131. 10.3233/jad-171032
28. Pascoal TA, Chamoun M, Lax E, Wey HY, Shin M, Ng KP, Kang MS, Mathotaarachchi S, Benedet AL, Therriault J, Lussier FZ, Schroeder FA, DuBois JM, Hightower BG, Gilbert TM, Zürcher NR, Wang C, Hopewell R, Chakravarty M, Savard M, Thomas E, Mohaddes S, Farzin S, Salaciak A, Tullo S, Cuello AC, Soucy JP, Massarweh G, Hwang H, Kobayashi E, Hyman BT, Dickerson BC, Guiot MC, Szyf M, Gauthier S, Hooker JM, Rosa-Neto P (2022) [(11)C]Martinostat PET analysis reveals reduced HDAC I availability in Alzheimer's disease. Nat Commun 13(1):4171. 10.1038/s41467-022-30653-5
29. Yang Z, Su W, Zhang Q, Niu L, Feng B, Zhang Y, Huang F, He J, Zhou Q, Zhou X, Ma L, Zhou J, Wang Y, Xiong W, Xiang J, Hu Z, Zhan Q, Yao B (2025) Lactylation of HDAC1 Confers Resistance to Ferroptosis in Colorectal Cancer. Adv Sci (Weinh) 12(12):e2408845. 10.1002/advs.202408845

30. Wu W, Wang X, Xu Y, Ma C, Qian X, Qiu W (2025) Neuropathological comorbidity, genetics and cognition in a Chinese community-based autopsy cohort. Brain 148(7):2481–2492. 10.1093/brain/awaf039
31. Gazestani V, Kamath T, Nadaf NM, Dougalis A, Burris SJ, Rooney B, Junkkari A, Vanderburg C, Pelkonen A, Gomez-Budia M, Valimaki NN, Rauramaa T, Therrien M, Koivisto AM, Tegtmeyer M, Herukka SK, Abdulraouf A, Marsh SE, Hiltunen M, Nehme R, Malm T, Stevens B, Leinonen V, Macosko EZ (2023) Early Alzheimer's disease pathology in human cortex involves transient cell states. Cell 186(20):4438–4453e4423. 10.1016/j.cell.2023.08.005
32. Shen W, Song Z, Zhong X, Huang M, Shen D, Gao P, Qian X, Wang M, He X, Wang T, Li S, Song X (2022) Sangerbox: A comprehensive, interaction-friendly clinical bioinformatics analysis platform. Imeta 1(3):e36. 10.1002/imt2.36
33. Alsema AM, Jiang Q, Kracht L, Gerrits E, Dubbelaar ML, Miedema A, Brouwer N, Hol EM, Middeldorp J, van Dijk R, Woodbury M, Wachter A, Xi S, Moller T, Biber KP, Kooistra SM, Boddeke E, Eggen BJL (2020) Profiling Microglia From Alzheimer's Disease Donors and Non-demented Elderly in Acute Human Postmortem Cortical Tissue. Front Mol Neurosci 13:134. 10.3389/fnmol.2020.00134
34. Chen JS, Wang HK, Su YT, Ho YC, Liang CL, Lee YK, Chu TH, Lin YS, Wu CC (2025) HDAC1 dysregulation promotes pro-inflammatory microglial activation and aggravates post-stroke neuroinflammation. Ann Med 57(1):2597624. 10.1080/07853890.2025.2597624
35. Wu Z, Bai Y, Qi Y, Chang C, Jiao Y, Bai Y, Guo Z (2023) HDAC1 disrupts the tricarboxylic acid (TCA) cycle through the deacetylation of Nur77 and promotes inflammation in ischemia-reperfusion mice. Cell Death Discov 9(1):10. 10.1038/s41420-023-01308-1
36. Sun W, Zhang N, Liu B, Yang J, Loers G, Siebert HC, Wen M, Zheng X, Wang Z, Han J, Zhang R (2022) HDAC3 Inhibitor RGFP966 Ameliorated Neuroinflammation in the Cuprizone-Induced Demyelinating Mouse Model and LPS-Stimulated BV2 Cells by Downregulating the P2X7R/STAT3/NF-kappaB65/NLRP3 Activation. ACS Chem Neurosci 13(17):2579–2598. 10.1021/acschemneuro.1c00826
37. Tao L, Yu W, Liu Z, Zhao D, Lin S, Szaloki D, Kicsak M, Kurtan T, Zhang H (2024) JE-133 Suppresses LPS-Induced Neuroinflammation Associated with the Regulation of JAK/STAT and Nrf2 Signaling Pathways. ACS Chem Neurosci 15(2):258–267. 10.1021/acschemneuro.3c00454
38. Liu H, Wang D, Feng X, Liu L, Liu B, Zhu L, Sun J, Zuo X, Chen S, Liu J, Xian J, Zhang C, Yang W (2025) Angelicin ameliorated ulcerative colitis through activating HDAC1-derived HIF-1alpha acetylation. Phytomedicine 140:156546. 10.1016/j.phymed.2025.156546
39. Zhang Y, Zhang X (2024) Virus-Induced Histone Lactylation Promotes Virus Infection in Crustacean. Adv Sci (Weinh) 11(30):e2401017. 10.1002/advs.202401017
40. Datta M, Staszewski O, Raschi E, Frosch M, Hagemeyer N, Tay TL, Blank T, Kreutzfeldt M, Merkler D, Ziegler-Waldkirch S, Matthias P, Meyer-Luehmann M, Prinz M (2018) Histone Deacetylases 1 and 2 Regulate Microglia Function during Development, Homeostasis, and Neurodegeneration in a Context-Dependent Manner. Immunity 48(3):514–529e516. 10.1016/j.immuni.2018.02.016

41. Wang L, Yu C, Tao Y, Yang X, Jiang Q, Yu H, Zhang J (2022) Transcriptome analysis reveals potential marker genes for diagnosis of Alzheimer's disease and vascular dementia. Front Genet 13:1038585. 10.3389/fgene.2022.1038585
42. Ralvenius WT, Mungenast AE, Woolf H, Huston MM, Gillingham TZ, Godin SK, Penney J, Cam HP, Gao F, Fernandez CG, Czako B, Lightfoot Y, Ray WJ, Beckmann A, Goate AM, Marcora E, Romero-Molina C, Ayata P, Schaefer A, Gjoneska E, Tsai LH (2023) A novel molecular class that recruits HDAC/MECP2 complexes to PU.1 motifs reduces neuroinflammation. J Exp Med 220(11). 10.1084/jem.20222105
43. Gupta R, Kumar P (2021) CREB1(K292) and HINFP(K330) as Putative Common Therapeutic Targets in Alzheimer's and Parkinson's Disease. ACS Omega 6(51):35780–35798. 10.1021/acsomega.1c05827
44. Rumbaugh G, Daws SE, Ozkan ED, Rojas CS, Hubbs CR, Aceti M, Kilgore M, Kudugunti S, Puthanveettil SV, Sweatt JD, Rusche J, Miller CA (2015) Pharmacological Selectivity Within Class I Histone Deacetylases Predicts Effects on Synaptic Function and Memory Rescue. Neuropsychopharmacology 40(10):2307–2316. 10.1038/npp.2015.93
45. Tian Q, Li J, Wu B, Pang Y, He W, Xiao Q, Wang J, Yi L, Tian N, Shi X, Xia L, Tian X, Chen M, Fan Y, Xu B, Tao Y, Song W, Du Y, Dong Z (2025) APP lysine 612 lactylation ameliorates amyloid pathology and memory decline in Alzheimer's disease. J Clin Invest 135(1). 10.1172/jci184656
46. Zhang X, Liu Y, Rekowski MJ, Wang N (2025) Lactylation of tau in human Alzheimer's disease brains. Alzheimers Dement 21(2):e14481. 10.1002/alz.14481
47. An X, He J, Xie P, Li C, Xia M, Guo D, Bi B, Wu G, Xu J, Yu W, Ren Z (2024) The effect of tau K677 lactylation on ferritinophagy and ferroptosis in Alzheimer's disease. Free Radic Biol Med 224:685–706. 10.1016/j.freeradbiomed.2024.09.021
48. Tao CC, Hsu WL, Ma YL, Cheng SJ, Lee EH (2017) Epigenetic regulation of HDAC1 SUMOylation as an endogenous neuroprotection against Aβ toxicity in a mouse model of Alzheimer's disease. Cell Death Differ 24(4):597–614. 10.1038/cdd.2016.161
49. Fei X, Chen L, Gao J, Jiang X, Sun W, Cheng X, Zhao T, Zhao M, Zhu L (2024) p53 lysine-lactylated modification contributes to lipopolysaccharide-induced proinflammatory activation in BV2 cell under hypoxic conditions. Neurochem Int 178:105794. 10.1016/j.neuint.2024.105794
50. Yang X, Chen YH, Liu L, Gu Z, You Y, Hao JR, Sun N, Gao C (2024) Regulation of glycolysis-derived L-lactate production in astrocytes rescues the memory deficits and Abeta burden in early Alzheimer's disease models. Pharmacol Res 208:107357. 10.1016/j.phrs.2024.107357
51. Wu Y, Yang L, Jiang W, Zhang X, Yao Z (2025) Glycolytic dysregulation in Alzheimer's disease: unveiling new avenues for understanding pathogenesis and improving therapy. Neural regeneration Res 20(8):2264–2278. 10.4103/NRR.NRR-D-24-00190
52. Lee JS, Yoon BS, Han S, Kim Y, Park CB (2025) Diminished lactate utilization in LDHB-deficient neurons leads to impaired long-term memory retention. Exp Neurol 384:115064. 10.1016/j.expneurol.2024.115064

53. Cao H, Liang J, Dong X, Xia Z, Luo X, Liu B (2026) Protein lactylation in Alzheimer's disease: bridging metabolism, pathology, and therapeutic opportunity. Front Aging Neurosci 18:1790090. 10.3389/fnagi.2026.1790090
54. Zhang D, Tang Z, Huang H, Zhou G, Cui C, Weng Y, Liu W, Kim S, Lee S, Perez-Neut M, Ding J, Czyz D, Hu R, Ye Z, He M, Zheng YG, Shuman HA, Dai L, Ren B, Roeder RG, Becker L, Zhao Y (2019) Metabolic regulation of gene expression by histone lactylation. Nature 574(7779):575–580. 10.1038/s41586-019-1678-1
55. Zhang D, Gao J, Zhu Z, Mao Q, Xu Z, Singh PK, Rimayi CC, Moreno-Yruela C, Xu S, Li G, Sin YC, Chen Y, Olsen CA, Snyder NW, Dai L, Li L, Zhao Y (2025) Lysine L-lactylation is the dominant lactylation isomer induced by glycolysis. Nat Chem Biol 21(1):91–99. 10.1038/s41589-024-01680-8
56. Ren H, Tang Y, Zhang D (2025) The emerging role of protein L-lactylation in metabolic regulation and cell signalling. Nat Metab 7(4):647–664. 10.1038/s42255-025-01259-0
57. Peng Y, Xiong RP, Wang B, Chen X, Ning YL, Zhao Y, Yang N, Zhang J, Li CH, Zhou YG, Li P (2025) c-Ski is a novel repressor of NF-kappaB through interaction with p65 and HDAC1 in U937 cells. Cell Commun Signal 23(1):165. 10.1186/s12964-025-02178-z

Figures

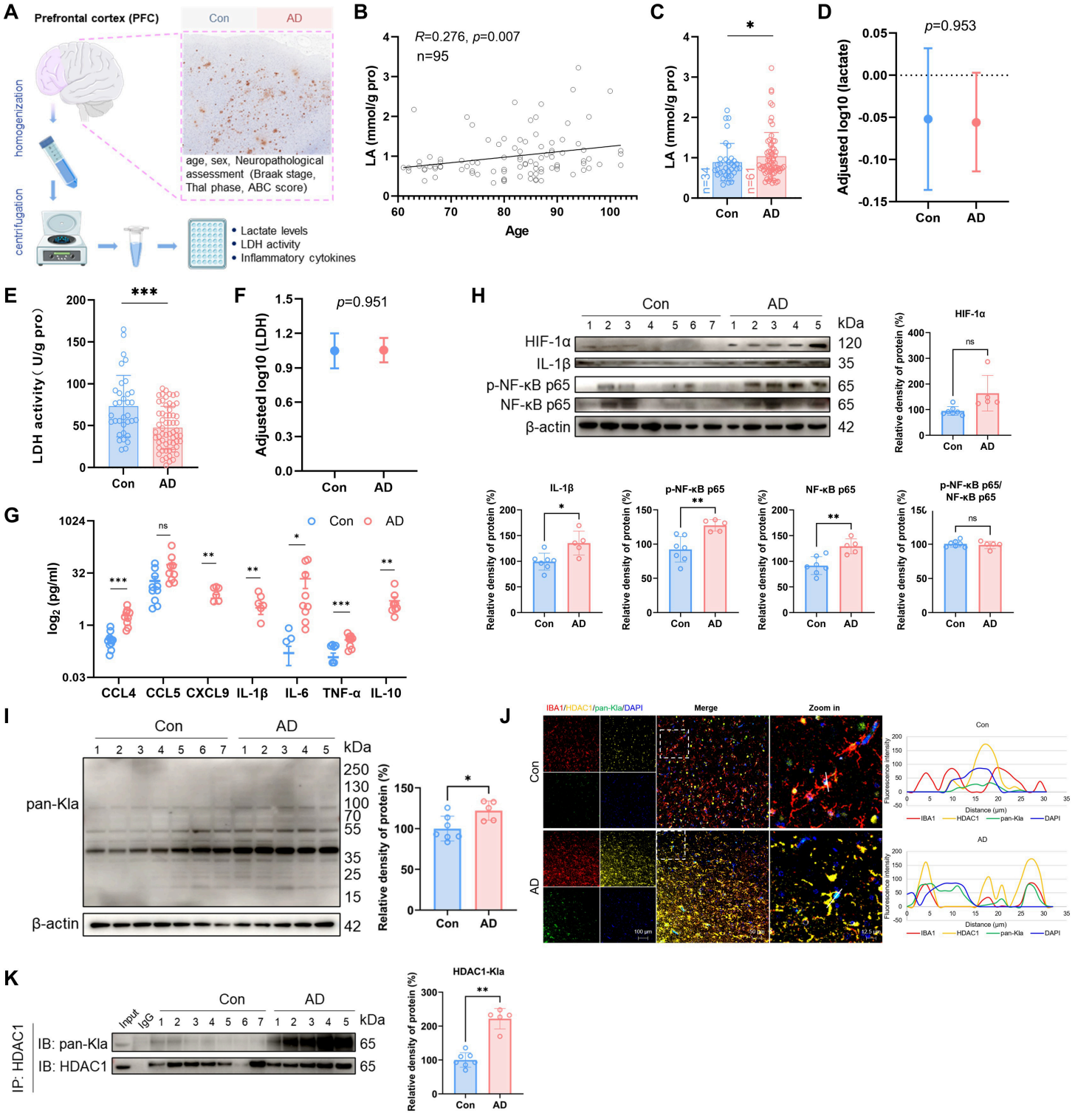


Figure 1

Brain lactate levels, inflammatory changes, and HDAC1 lactylation in AD prefrontal cortex.

(A) Postmortem prefrontal cortex tissues from control and AD subjects were homogenized and centrifuged; supernatants were collected for lactate concentration and LDH activity measurements. **(B)** Correlation between prefrontal cortex lactate levels and age across the entire cohort. **(C)** Comparison of prefrontal cortex lactate levels between control and AD donors. **(D)** Age-adjusted comparison of lactate

levels between control and AD donors using ANCOVA. Data points represent estimated marginal means (EMMs), and error bars indicate 95% confidence intervals (CIs). **(E)** Comparison of LDH activity between control and AD donors. **(F)** Age-adjusted comparison of LDH activity between control and AD donors using ANCOVA. Data points represent EMMs, and error bars indicate 95% CIs. **(G)** Quantification of inflammatory cytokines and chemokines (CCL4, CXCL9, IL-1β, IL-6, TNF-α, and IL-10) in prefrontal cortex homogenates from control and AD donors. **(H)**Representative immunoblots and densitometric analyses of HIF-1α, IL-1β, phospho-NF-κB p65 (Ser536), and total p65 in control and AD prefrontal cortex. **(I)** Representative immunoblot and quantification of global protein lactylation (pan-Kla). **(J)** Representative immunofluorescence staining of IBA1 (red), HDAC1 (yellow), pan-Kla (green), and DAPI (blue) in control and AD prefrontal cortex; right panels display fluorescence intensity profiles along the indicated lines. **(K)** Immunoprecipitation of HDAC1 from prefrontal cortex lysates, followed by immunoblotting with anti-Kla antibody and densitometric quantification. Data are presented as mean ± SD, except for age-adjusted EMMs, which are shown with 95% CIs. *$p < 0.05$, **$p < 0.01$, ***$p< 0.001$; ns, not significant.

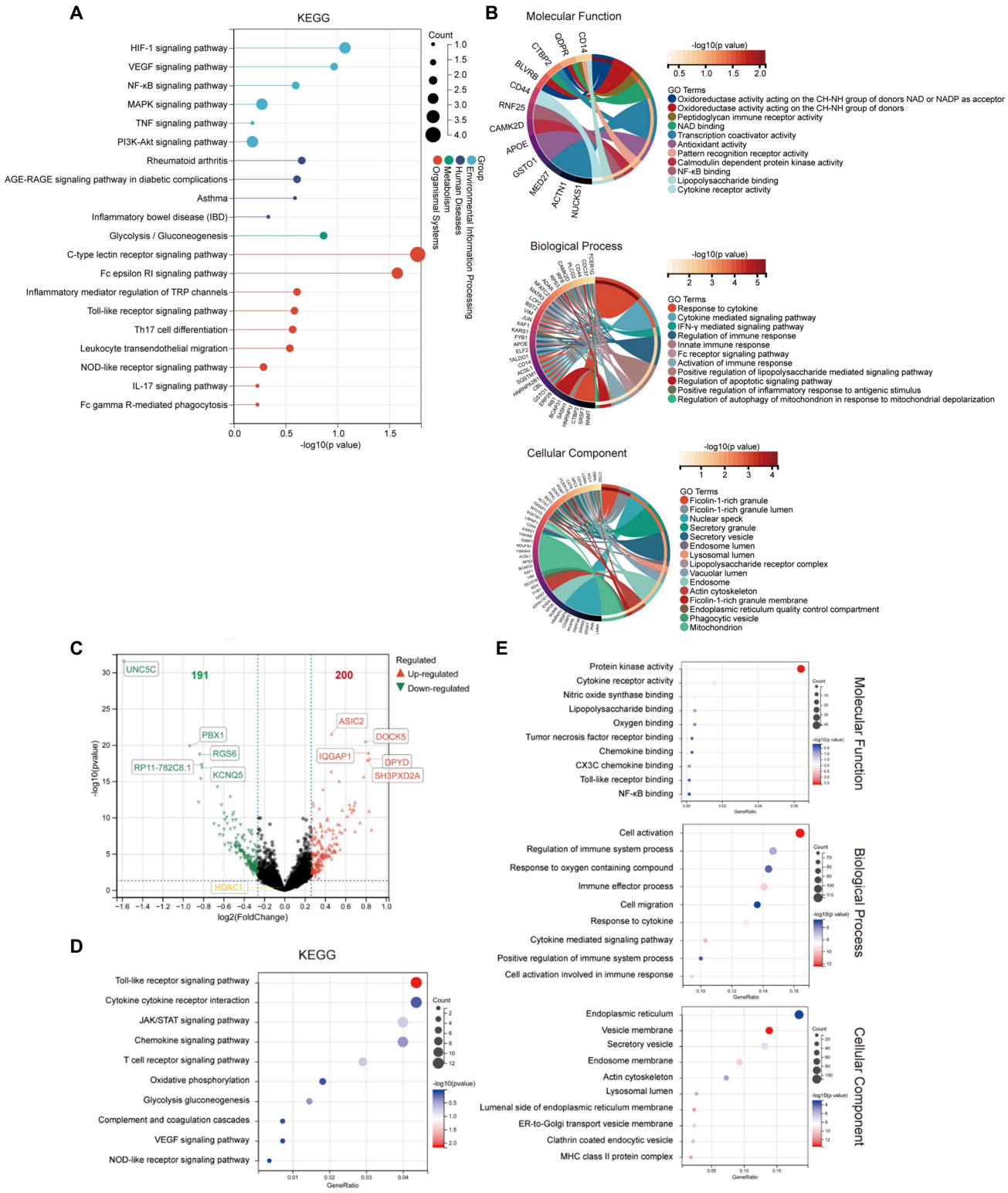


Figure 2

AD-associated microglia exhibit a conserved immune-metabolic transcriptional program across cortical regions. Panels A and B are derived from microglial single-cell RNA-seq data of early AD cortex [33]; panels C-E are from independent microglial datasets of superior frontal gyrus and parietal cortex of AD and non-demented elderly donors [31]. **(A)** KEGG pathway enrichment of differentially expressed proteins in AD microglia. **(B)** GO enrichment of Molecular Function, Biological Process, and Cellular

Component categories. **(C)** Volcano plot of differentially expressed proteins, with upregulated (red, n=200) and downregulated (green, n=191) proteins ($p < 0.05$, fold change >1.5); top five upregulated and downregulated genes are labeled. **(D)** KEGG enrichment of upregulated proteins. **(E)** Dot plot of GO categories for upregulated proteins; bubble size represents protein count, and color represents −log10(p).

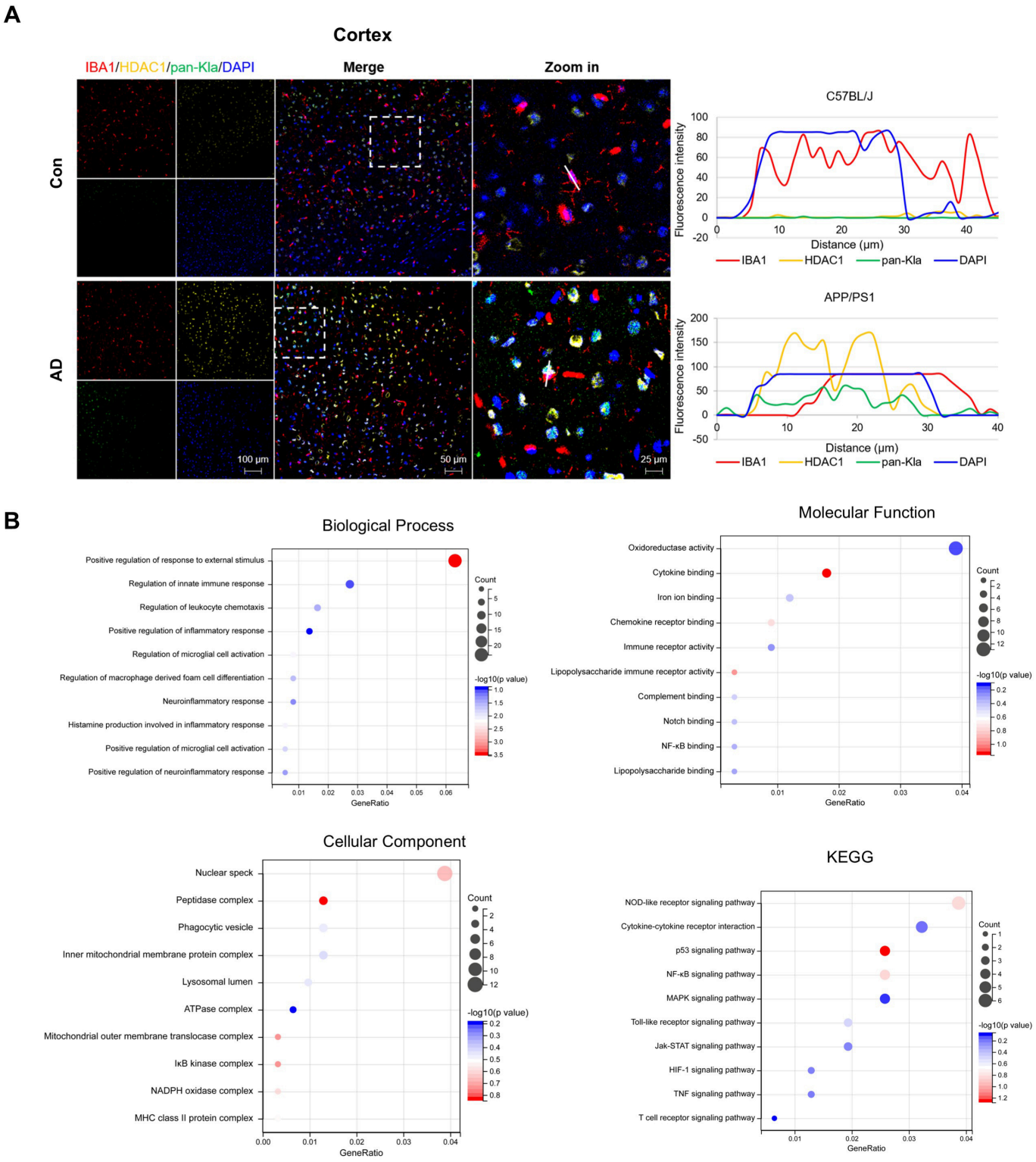


Figure 3

HDAC1 lactylation is increased in activated microglia and associates with inflammatory programs in AD mice. (A) Immunofluorescence staining of IBA1 (red), HDAC1 (yellow), pan-Kla (green), and DAPI (blue) in cortical sections from 5×FAD and WT mice; right panels display fluorescence intensity profiles along the indicated lines. **(B)**GO and KEGG enrichment analyses of upregulated microglial proteins in 5×FAD mice show activation of inflammatory, cytokine, and chemokine signaling pathways. Data are mean ± SD; *$P < 0.05$.

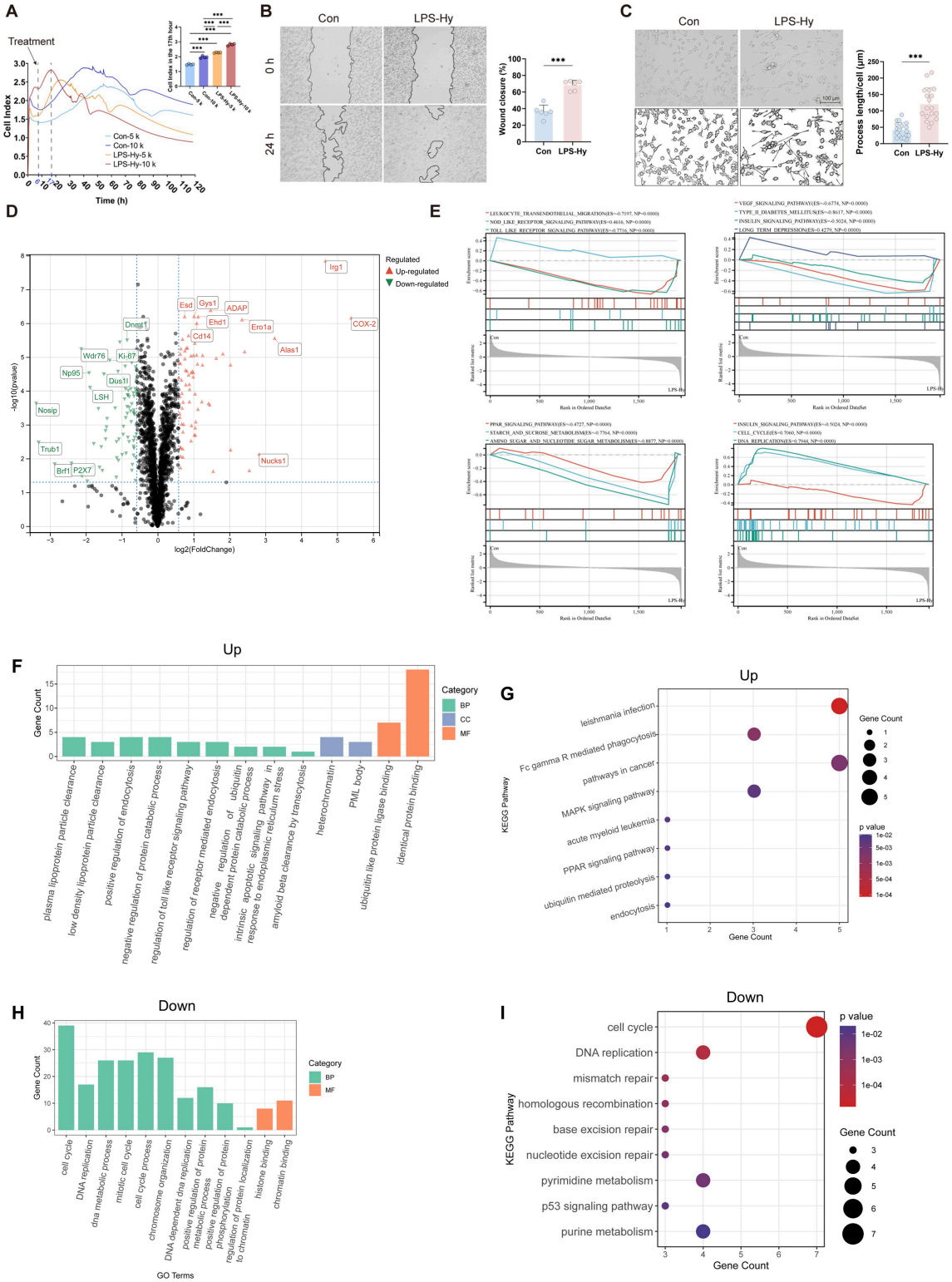


Figure 4

Hypoxic inflammatory stimulation induces AD-like microglial proteomic reprogramming. (A) Real-time impedance monitoring of BV2 microglia seeded at 5×10³ cells/mL (5K) or 1×10⁴ cells/mL (10K) under control, LPS, hypoxia, and LPS-Hy conditions. Cell index was continuously recorded following stimulation at 6 h post-seeding. Right panel shows cell index values at 17 h post-seeding. **(B)** Wound-healing assay of BV2 microglia under control and LPS-Hy conditions. Representative images at 0 h and 24 h are shown together with quantification of wound closure. **(C)** Morphological assessment of BV2 microglia under control and LPS-Hy conditions, with representative bright-field images, traced cell processes, and quantification of process length. **(D)** Volcano plot showing differentially expressed proteins in BV2 microglia following LPS-Hy stimulation; upregulated (red) and downregulated (green) proteins are indicated. **(E)** GSEA of LPS-Hy-regulated proteins. **(F)** GO enrichment analysis of upregulated proteins, with Biological Process, Molecular Function, and Cellular Component categories. **(G)** KEGG pathway enrichment analysis of upregulated proteins. **(H)** GO enrichment analysis of downregulated proteins, with Biological Process, Molecular Function, and Cellular Component categories. **(I)** KEGG pathway enrichment analysis of downregulated proteins. Data are mean ± SD. Statistical significance was determined using Student's t-test as appropriate. ***$p < 0.001$.

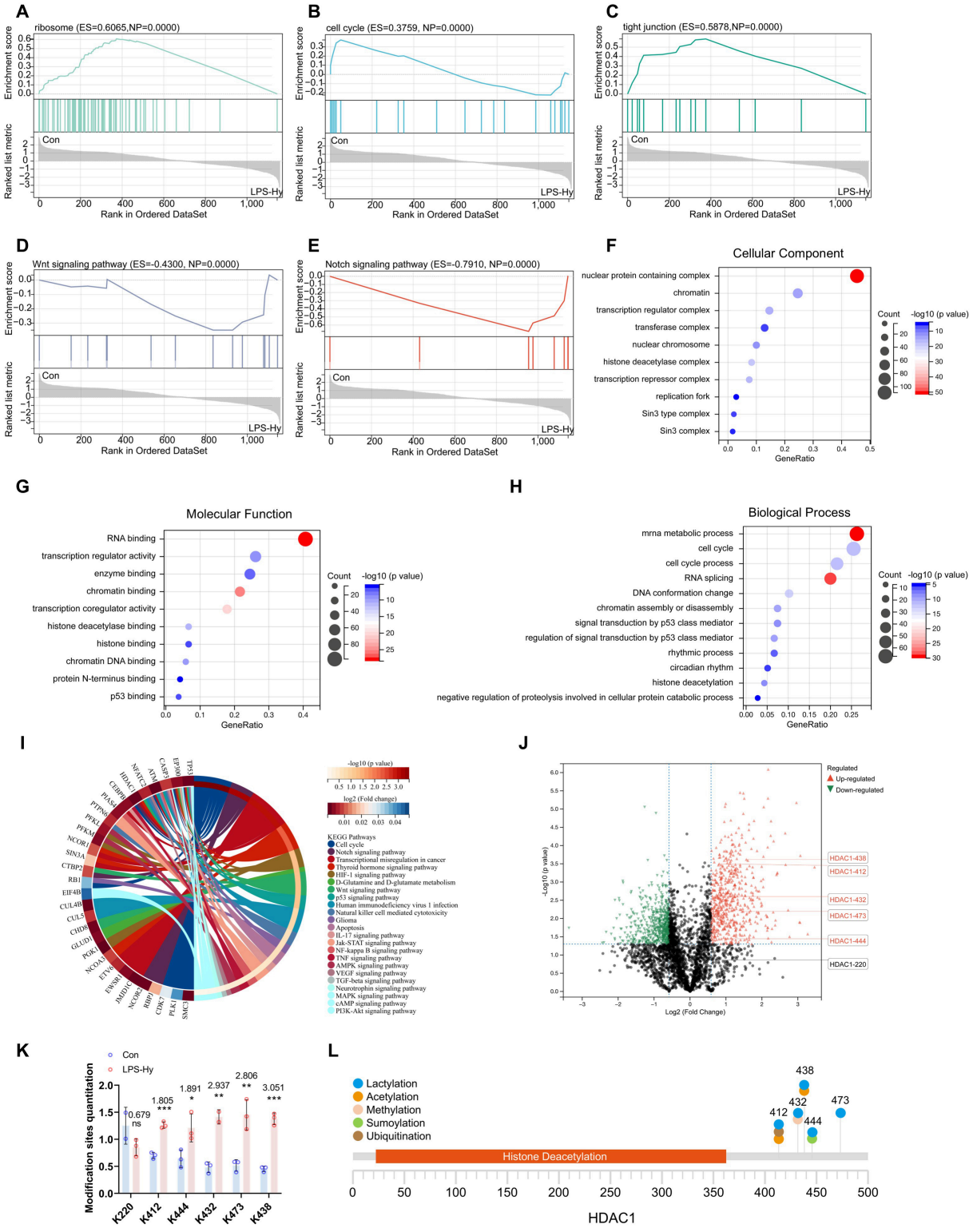


Figure 5

Lactylome profiling identifies HDAC1 K438 as a candidate regulatory lactylation site in microglial reprogramming. (A-E) GSEA of lactylated proteins in BV2 microglia following LPS-Hy treatment, with enrichment categories including ribosome biogenesis, protein translation, cytoskeletal organization, tight junction regulation, Wnt signaling, and Notch signaling pathways. **(F-H)** GO enrichment analysis of upregulated lactylated proteins. **(I)** KEGG pathway enrichment analysis of upregulated lactylated

proteins. **(J)** Volcano plot of HDAC1 lactylated lysine residues detected in BV2 microglia following LPS-Hy treatment; each point represents an identified lactylation site on HDAC1. **(K)** Quantification of HDAC1 lactylation at lysine residues K412, K432, K438, K444, and K473 in BV2 microglia following LPS-Hy treatment; numbers above bars indicate fold change values relative to control. **(L)** Structural representation of HDAC1 protein based on PhosphoSitePlus annotation, with reported post-translational modification sites and mapped lactylation residues indicated. Data are mean ± SD; *$p < 0.05$, **$p < 0.01$, ***$p < 0.001$; ns, not significant.

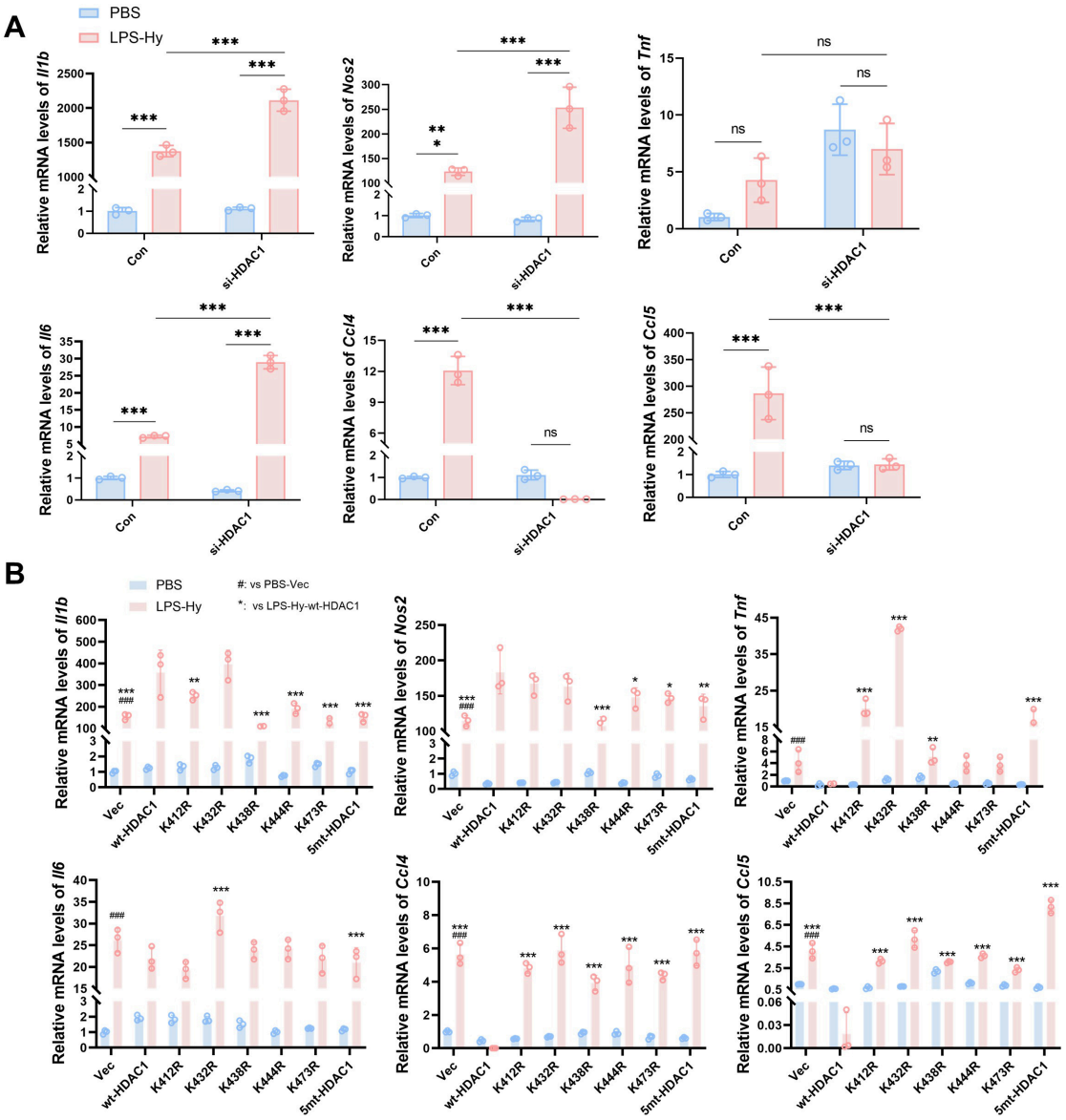
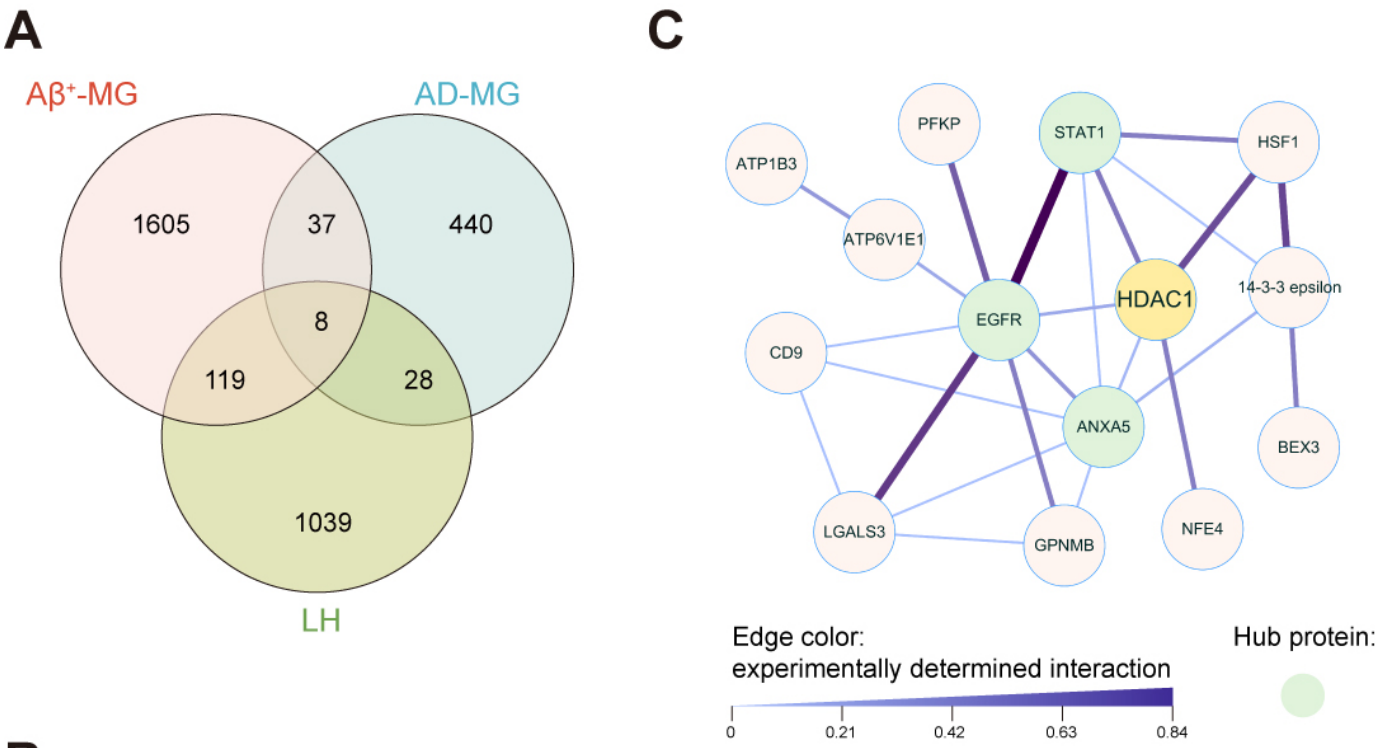


Figure 6

HDAC1 K438 lactylation regulates NF-κB-mediated inflammatory activation in microglia. (A) Relative mRNA expression of *Il1b*, *Nos2*, *Tnf*, *Il6*, *Ccl4*, and *Ccl5* in control or HDAC1-knockdown BV2 cells following PBS or LPS-Hy treatment, as determined by rtPCR. **(B)** Relative mRNA expression of inflammatory genes in BV2 cells expressing wild-type HDAC1 or K438R mutant constructs following LPS-Hy treatment. **(C)** Immunoblot analysis of phosphorylated NF-κB p65 (p-p65) and total p65 in BV2 cells expressing wild-type or K438R mutant HDAC1 following LPS-Hy treatment. **(D)** IP of Flag-tagged HDAC1 from BV2 cells expressing wild-type or K438R mutant constructs following LPS-Hy treatment, followed by immunoblotting with anti-Flag and anti-pan-Kla antibodies. Data are mean ± SD; $*p < 0.05$, $**p < 0.01$, $***p < 0.001$; ns, not significant.



B

Core Factor	Change				Main Biological Function
	AD-MG	Aβ+-MG	LH-MS	LH-Kla	
ATP1B3	Up	Up	Down	Up	Sodium/potassium ATPase subunit; maintains ion homeostasis
ATP6V1E1	Up	Down	Up	Down	Subunit of vacuolar ATPase; essential for lysosomal acidification and autophagy
CD9	Up	Up	Up	Down	Tetraspanin involved in cell adhesion, migration, and microglial activation
GPNMB	Up	Up	Down	Down	Transmembrane glycoprotein; promotes inflammation and phagocytosis
LGALS3	Up	Up	Up	Down	β-galactoside-binding lectin; pro-inflammatory and phagocytic functions
PFKP	Up	Up	Up	Up	Rate-limiting enzyme of glycolysis; converts F6P to FBP
STAT1	Down	Up	Up	Down	Transcription factor for interferon-γ signaling; promotes pro-inflammatory gene expression
14-3-3 epsilon	Down	Down	Up	Down	Phosphoserine-binding adaptor; regulates cell signaling and apoptosis

Figure 7

Conserved microglial module with HDAC1-linked regulation in AD and inflammatory stress. (A) Venn diagram of overlapping factors identified from AD-associated microglia (AD-MG) [33], Aβ-positive microglia (Aβ+-MG) [31], and BV2 microglia exposed to LPS-Hy. **(B)** Expression patterns and annotated biological functions of the eight intersecting genes (ATP1B3, ATP6V1E1, CD9, GPNMB, LGALS3, PFKP, STAT1, and 14-3-3 epsilon) across Aβ+-MG, AD-MG, BV2 LPS-Hy proteomic dataset (LH-MS), and BV2

lactylation dataset under LPS-Hy (LH-Kla). **(C)** PPI network seeded with the eight conserved core genes and expanded via STRING. Green nodes (STAT1, EGFR, and ANXA5) denote top core factors identified by cytoHubba in Cytoscape. HDAC1 was not pre-weighted but emerged as a highly connected node. Edge thickness and color indicate experimentally determined interaction confidence.

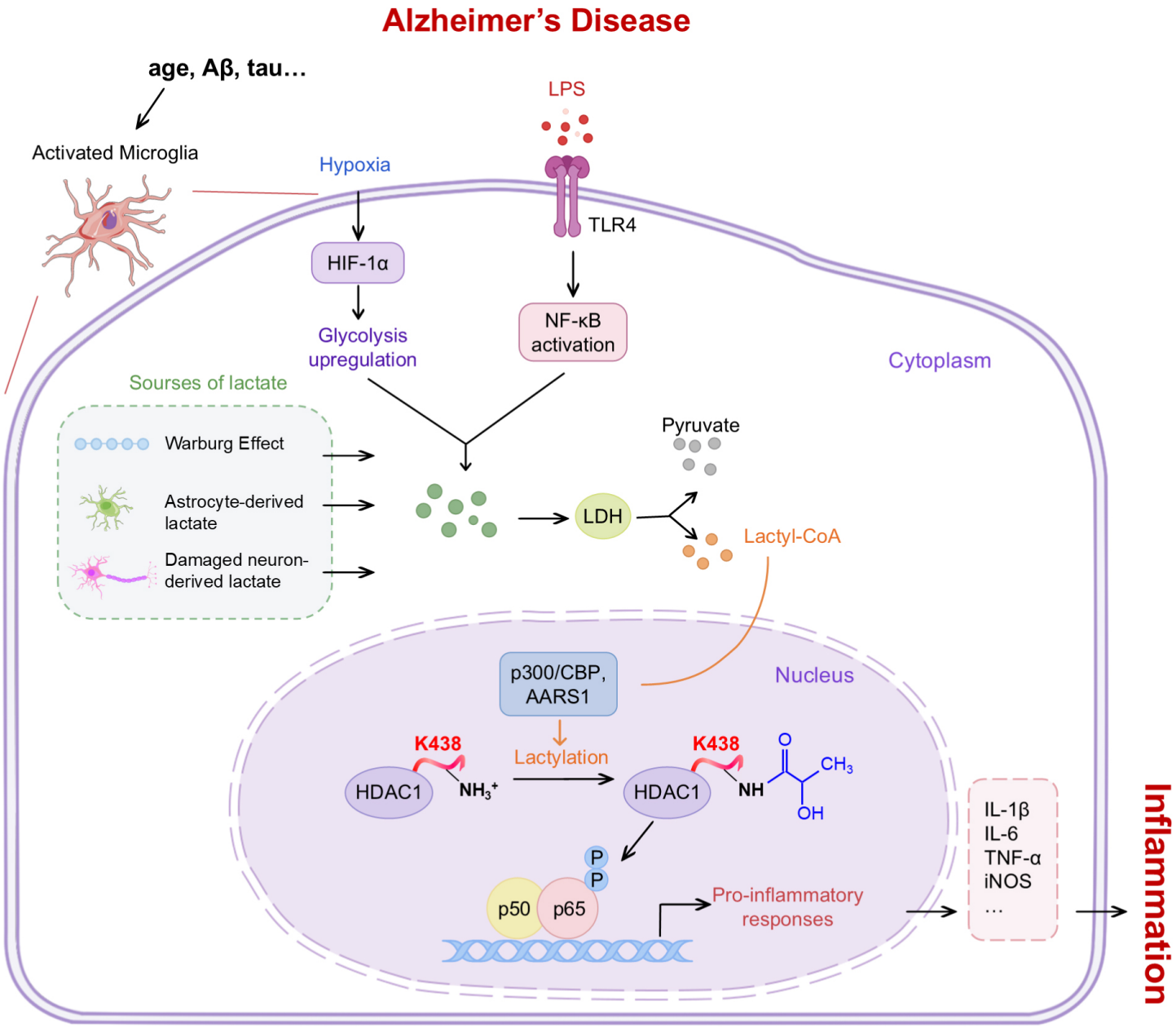


Figure 8

HDAC1 K438 lactylation-mediated regulation of inflammatory microglial activation in AD. under hypoxic-inflammatory stress, microglia undergo glycolytic activation with increased lactate production; lactate is converted to lactyl-CoA, serving as the acyl donor for p300/CBP or AARS1-dependent lactylation; HDAC1 undergoes K438 lactylation, which modulates HDAC1-p65 interaction, enhances p65-driven transcriptional activity, and promotes pro-inflammatory mediator expression.

Supplementary Files

This is a list of supplementary files associated with this preprint. Click to download.

- Stable.1.xlsx
- Stable.2.xlsx
- Fig.S1.jpg
- Fig.S2.jpg
- Fig.S3.jpg
- Fig.S4.jpg
- Fig.S5.jpg